J. Fluid Mech. (2001), *vol.* 440, *pp.* 293–326. Printed in the United Kingdom

Three-dimensional theory of water impact. Part 1. Inverse Wagner problem

By Y.-M. SCOLAN[1] AND A. A. KOROBKIN[2]

[1]Ecole Supérieure d'Ingénieurs de Marseille, 13451 Marseille Cedex 20, France

[2]Lavrentyev Institute of Hydrodynamics, Novosibirsk 630090, Russia

(Received 12 June 2000 and in revised form 14 February 2001)

The three-dimensional problem of blunt-body impact onto the free surface of an ideal incompressible liquid is considered within the Wagner theory. The theory is formally valid during an initial stage of the impact. The problem has been extensively studied in both two-dimensional and axisymmetric cases. However, there are no exact truly three-dimensional solutions of the problem even within the Wagner theory. At present, three-dimensional effects in impact problems are mainly handled approximately by using a sequence of two-dimensional solutions and/or aspect-ratio correction factor. In this paper we present exact analytical rather than approximate solutions to the three-dimensional Wagner problem. The solutions are obtained by the inverse method. In this method the body velocity and the projection on the horizontal plane of the contact line between the liquid free surface and the surface of the entering body are assumed to be given at any time instant. The shape of the impacting body is determined from the Wagner condition. It is proved that an elliptic paraboloid entering calm water at a constant velocity has an elliptic contact line with the free surface. Most of the results are presented for elliptic contact lines, for which analytical solutions of the inverse Wagner problem are available. The results obtained can be helpful in testing other numerical approaches and studying the influence of three-dimensional effects on the liquid flow and the hydrodynamic loads.

1. Introduction

In spite of increasing needs of industry, the three-dimensional impact problem is far from being solved yet. Accurate numerical methods to solve the problem even within the Wagner approximation are urgently required, in particular by ship designers to properly evaluate the impact loads in severe sea conditions. Real impact processes are three-dimensional in nature and estimations of the loads from strip theory may not be accurate enough, especially close to the ship's bow where impact mainly occurs. The initial stage of the impact is of particular interest. This stage, during which the hydrodynamic loads take their maximum values, gives estimates necessary for the dynamic-strength calculation of an impacting structure and supplies the initial data for further numerical calculations of the three-dimensional hydrodynamic problem.

The three-dimensional unsteady problem of liquid flow due to the impact of a blunt body onto the liquid free surface is considered here. Initially the liquid is at rest and occupies the lower half-space, $z < 0$, and the rigid body touches the liquid free surface, $z = 0$, at a single point. This point is taken as the origin of the Cartesian coordinate system $Oxyz$. At some instant of time, taken as initial ($t = 0$), the body starts to penetrate the liquid vertically with the body velocity $U(t)$ being prescribed.

The position of the entering body at any time instant t is given by the equation $z = f(x, y) - h(t)$, where the function $f(x, y)$ describes the body shape, $f(0, 0) = 0$ and $|\nabla f| \ll 1$ close to the impact point, and $h(t)$ is the penetration depth of the body, $h(0) = 0$ and $h_{,t} = U(t)$. External mass forces and surface tension are neglected. The liquid is assumed to be ideal and incompressible, and its flow three-dimensional and irrotational.

The domain occupied by the liquid changes in time. At any instant $t > 0$ the liquid boundary consists of the free surface and the wetted part of the entering body, which are separated by the contact line. The contact region starts to grow from a single point, implying that the topology of the liquid boundary changes at the impact instant, $t = 0$.

The main objectives of the water impact problem are to determine the liquid flow, the pressure distribution and the geometry of the flow region; the shape of the entering body and the law of the body motion are given. The problem is very complicated since the flow domain and the division of its boundary into the free surface and contact region components are unknown in advance and have to be determined together with the fluid flow and the pressure distribution.

1.1. *Wagner approximation*

The problem can be greatly simplified if we restrict ourselves to the initial stage of the interaction only and additionally assume that the entering body is blunt. This means that the body shape close to the initial contact point, $x = 0$, $y = 0$, has a small deadrise angle, $|\nabla f(x, y)| \ll 1$; this is the main assumption of Wagner's theory (Wagner 1932). During the initial stage of a blunt-body impact the dimensions of the wetted area in the horizontal directions are much greater than the penetration depth $h(t)$. This implies that the wetted part of the body can be approximated at the leading order by an equivalent flat disk. In addition, the free surface elevation is of the same order as $h(t)$, which makes it possible to linearize the boundary conditions and to impose them on the initially undisturbed liquid level at the leading order as $t \to 0$. This procedure assumes, in particular, that the free surface position can be projected one-to-one onto the plane $z = 0$ and be described for small times by the equation

$$z = \eta(x, y, t). \tag{1.1}$$

It is well-known that for blunt-body impact this statement is not correct due to the spray jet that forms at the periphery of the contact region. On the other hand, it is also known that the thickness of the spray jet is small and the jetting makes a negligible contribution to the flow pattern, but the jet energy has to be taken into account in the analysis of energy redistribution during the water impact (see Korobkin 1994). Therefore, at the leading order as $t \to 0$ the spray jet can be ignored in the analysis of both the free surface elevation and the fluid flow outside a small vicinity of the jet root region. Within the Wagner theory the contact line plays the most important role; this needs to be clarified. Its definition follows from equation (1.1), which is valid outside the jet root region. For blunt bodies the dimension of this region during the initial stage is much smaller than the dimension of the contact area. Moreover, the elevation of this region above the plane $z = 0$ is of the order of the penetration depth $h(t)$, which is also much smaller than the horizontal dimension of the contact region. This implies that the position of the moving jet root region is close to the corresponding curve on the plane $z = 0$. This curve is considered as the contact line in the Wagner approach and is denoted $\Gamma(t)$. The notation used in the

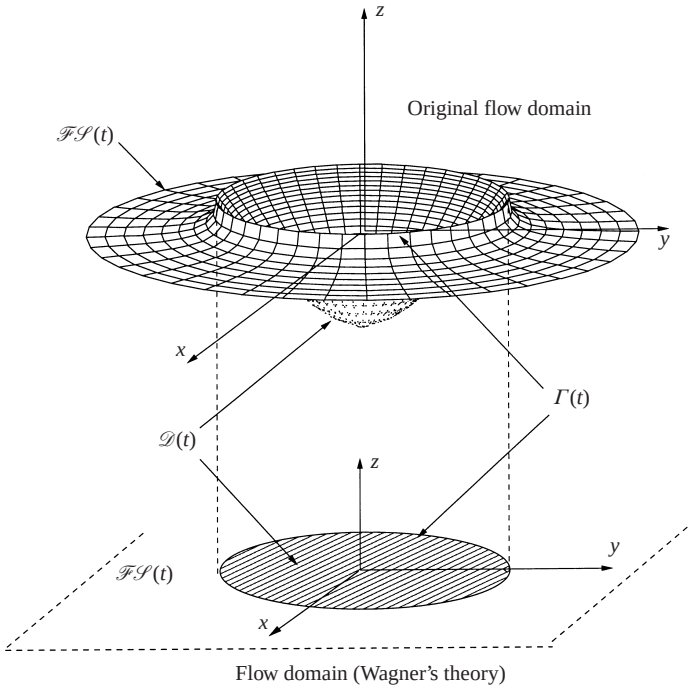

FIGURE 1. Sketches of three-dimensional flow pattern for normal penetration of a blunt body into a liquid within the original problem and within the Wagner approximation: $\mathscr{D}(t)$, contact region; $\mathscr{FS}(t)$, liquid free surface; $\Gamma(t)$, contact line. In the physical domain the spray jet and the dry part of the body are not shown.

following developments concerning the different parts of the flow boundaries, is given in figure 1.

Wagner (1932) observed that the vertical distance between the liquid free surface, $\eta(x, y, t)$, and the surface of the moving body, $f(x, y) - h(t)$, inside the jet root region, $(x, y) \in \Gamma(t)$, is of the same order as the thickness of the spray jet and tends to zero as $t \to 0$. At the leading order he arrived at the equation

$$\eta(x, y, t) = f(x, y) - h(t), \quad (x, y) \in \Gamma(t), \tag{1.2}$$

which is now referred to as the Wagner condition. Within the Wagner theory the closed curve $\Gamma(t)$ divides the liquid boundary, $z = 0$, into two parts; the outer and inner parts correspond to the free surface $\mathscr{FS}(t)$ and contact region $\mathscr{D}(t)$, respectively.

Within the Wagner theory the boundary conditions are linearized and imposed on the undisturbed liquid surface $z = 0$, and the liquid motion is irrotational and is described by the velocity potential $\phi(x, y, z, t)$. The potential $\phi(x, y, z, t)$ is a harmonic function in the lower half-space, $z < 0$, is identically zero for $t < 0$ and satisfies mixed boundary conditions on the plane $z = 0$. It satisfies the linearized free surface conditions. On the free surface of the liquid, $z = 0$ and $(x, y) \in \mathscr{FS}(t)$, the dynamic and kinematic conditions are $\phi = 0$ and $\eta_{,t} = \phi_{,z}$ respectively. In the contact region, $z = 0$ and $(x, y) \in \mathscr{D}(t)$, the linearized boundary condition is $\phi_{,z} = -U(t)$. The position of the contact region $\mathscr{D}(t)$ is determined with the help of the Wagner condition (1.2) provided that the functions $f(x, y)$ and $h(t)$ are given. In order to close this elliptic boundary value problem, the far-field condition implying that the velocity potential vanishes as $x^2 + y^2 + z^2 \to \infty$ is used. It should be noted that

(i) the velocity potential is continuous through the contact line $\Gamma(t)$ and (ii) the formulated Wagner problem is nonlinear even though both the equations of liquid motion and the boundary conditions are linear. Nonlinearity of the problem comes from equation (1.2).

In order to obtain in practice a solution of the Wagner problem in a time interval $[0, t_1]$, one usually assumes that the contact lines $\Gamma(\tau)$, where $\tau \in [0, t_1]$, are known. Then the velocity potentials $\phi(x, y, z, \tau)$ can be calculated as the solutions of the mixed boundary value problem for the Laplace equation in the lower half-space, $z < 0$, with τ now being a parameter. As a result, the vertical velocities $\phi_{,z}(x, y, 0, \tau)$ of the free surface are calculated. The time integration of the linearized kinematic condition $\eta_{,\tau}(x, y, \tau) = \phi_{,z}(x, y, 0, \tau)$, where $(x, y) \in \mathscr{F}\mathscr{S}(\tau)$, from 0 to t provides the elevation which is finally introduced into the Wagner condition (1.2). In order to satisfy equality (1.2), it is clear that the lines $\Gamma(\tau)$, where $\tau \in [0, t]$, cannot be arbitrary and have to be determined together with the liquid flow. We expect that the contact line $\Gamma(t)$ can be determined uniquely for smooth blunt bodies but this has not yet been proved. Mathematical analysis of the well-posedness of the Wagner problem is urgently required. The regularity properties of the solutions must be taken into account for developing accurate numerical algorithms.

1.2. *Early research work*

The Wagner problem is usually solved numerically by a time-marching scheme iterating at each given instant (see, for example, Donguy, Peseux & Fontaine 2000). For three-dimensional configurations this algorithm rapidly becomes time consuming since one has to iterate over a continuous curve in the plane $z = 0$. The results may be expected to be either very expensive or of poor accuracy. The most CPU time demanding task is the velocity potential solution for a given but, in general, complicated contact line $\Gamma(t)$.

Different approaches have been proposed to solve the three-dimensional impact problem with a Wagner formulation. One of them is formulated in terms of a variational inequality (Korobkin 1982). This approach has been formulated for three-dimensional configurations and provides an easily implemented algorithm for carrying out numerical calculations. It has the added bonus of providing a framework for discussion of the existence, uniqueness and regularity properties of the weak solution of the model. A minimization algorithm for numerical solution of the variational inequality was used by Howison, Ockendon & Wilson (1991) in the case of two-dimensional wedge impact. Good agreement with the exact analytical solution was reported even with rough finite-element discretization. The three-dimensional entry problem was treated with the help of this approach by Takagi (1997). The particular problem of a cone entry was solved, and good agreement with the available analytical solution reported. The approach was extended by Takagi (1997) to account for the air cushion effect. Several three-dimensional shapes were tested. Difficulties with evaluation of the total hydrodynamic force on the entering body within this approach were recognized and reported. These difficulties were successfully resolved recently by Donguy *et al.* (2000).

Other approaches introduced by Meyerhoff (1970) and Watanabe (1986*a*, *b*, 1987) are described in § 3. In the case of elongated bodies such as a long ship, strip theory, which is very popular in ship hydrodynamics, can be used to obtain an approximate solution of the three-dimensional impact problem. Within strip theory the three-

dimensional process is approximated by a sequence of two-dimensional impacts of each body cross-section.

1.3. *Inverse method in the Wagner problem*

In order to estimate the accuracy of different approximate approaches and also to supply exact solutions of the Wagner problem, the inverse method is used in the present analysis. In this method the position of the contact line $\Gamma(t)$ is assumed known at any time instant and the Wagner condition (1.2) is considered as the formula for the entering body shape. It is worth noting that the symmetric plane problem of blunt-body impact was originally solved by using the inverse method (Wagner 1932). In fact, in the plane case the vertical velocity of the free surface is given in analytical form but the free surface elevation is not. Wagner assumed that the penetration depth h is a polynomial of the contact region dimension. Coefficients of this polynomial are unknown in advance and are calculated from equation (1.2). This method leads to exact solutions provided that the body shape is also described by a polynomial. The same idea has been used by Schmieden (1953) to solve the axisymmetric impact problem. Borodich (1988) used this method for three-dimensional and self-similar impact configurations, and considered elliptic contact lines as an example. In this case the distribution of the vertical velocity on the free surface is given analytically as in both the plane and axisymmetric problems. However the final results are still complicated and are not easy to analyse. Unfortunately, no calculations were performed and, in particular, it was impossible to confirm the previous results by Korobkin (1985) who supposed that an elliptic paraboloid provides an elliptic contact region (see also Korobkin & Puchnachov 1988). This is demonstrated in the present paper starting from the pioneering work of Borodich (1988). Toyama (1996) also proposed quasi-exact solutions of the direct Wagner problem for an impacting ellipsoid.

To our knowledge, all three-dimensional solutions of the Wagner problem provided so far are approximate, even for the simplest case of an elliptic contact region. In the present paper exact solutions for an elliptic paraboloid and a cone are presented for the first time. Approximate solutions published before are tested against these exact solutions. The way to produce more exact solutions is described. The solutions obtained make it possible to analyse the influence of the three-dimensional effects on the liquid flows and loads caused by impact. The results presented are of interest not only for a ship-building audience but also for specialists from many other fields (material science, energetics, agriculture and so on), who deal with three-dimensional liquid/solid impact problems in different configurations like rigid body impact onto a liquid free surface, liquid drop impact onto a rigid surface and jet impact.

The formulation of the most general inverse Wagner problem is presented in § 2. Section 3 describes the method of solution of the inverse problem. Special attention is paid to the numerical algorithms to solve the mixed boundary-value problem for the Laplace equation. The inverse method generalizes the method introduced by Wagner (1932) to solve the plane impact problem. Applications to elliptic contact region are studied in § 4. The impact problem for elliptic regions both homothetically and non-homothetically expanding in time is considered in § 5. Exact analytical solutions of the Wagner problem and their application are studied in § 6. The applicability of the strip theory is analysed, in particular with the help of the exact solution obtained for the elliptic paraboloid entry problem. Finally in § 7 the results obtained are summarized and some directions of further research in the field of three-dimensional Wagner problem are outlined.

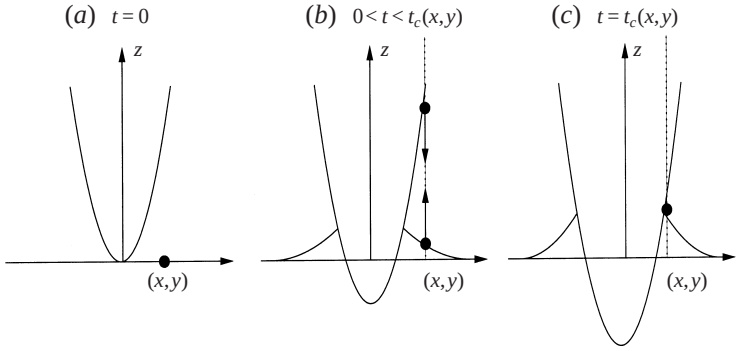

FIGURE 2. Three successive steps of the free surface elevation at location (x, y) during slamming up to time instant of contact $t_c(x, y)$: (*a*) initial time, (*b*) intermediate time instant and (*c*) instant of the contact.

2. Formulation of the inverse problem

Within the Wagner theory, the linearized dynamic condition imposes that fluid particles of the free surface can move only vertically. Such a particle which is initially at location $(x, y, 0)$ reaches the entering body surface at a time instant denoted by $t_c(x, y)$; it is clear that $t_c(0, 0) = 0$. A simplified two-dimensional illustration of the entry process with the definition of the function $t_c(x, y)$ is given in figure 2, where three successive steps of the process are drawn. If the function $t_c(x, y)$ is known in advance, the contact line $\Gamma(t)$ is defined by the equation (Howison *et al.* 1991)

$$t = t_c(x, y), \tag{2.1}$$

and the contact region is $\mathscr{D}(t) = \{x, y | t_c(x, y) < t\}$. Equation (2.1) determines a three-dimensional surface in the space with coordinates x, y and t, a cross-section $t = \tau$ of which provides the contact line $\Gamma(\tau)$ at the time instant τ. The elevation of the fluid particle with initial coordinates $(x, y, 0)$ at the time instant $t_c(x, y)$ above the initial water level can be found either from the linearized kinematic boundary condition

$$\eta(x, y, t_c(x, y)) = \int_0^{t_c(x,y)} \phi_{,z}(x, y, 0, \tau)\, \mathrm{d}\tau \tag{2.2}$$

or from the Wagner equation (1.2)

$$\eta(x, y, t_c(x, y)) = f(x, y) - h(t_c(x, y)). \tag{2.3}$$

The vertical velocity $\phi_{,z}(x, y, 0, \tau)$ in (2.2) follows from the solution of the boundary value problem for the velocity potential $\phi(x, y, z, \tau)$

$$\left.\begin{array}{lll} \Delta\phi = 0 & & z < 0, \\ \phi = 0 & & \text{on } \mathscr{F}\mathscr{S}(\tau), \\ \phi_{,z} = -U(\tau) & & \text{on } \mathscr{D}(\tau), \\ \phi \to 0 & & (x^2 + y^2 + z^2) \to \infty. \end{array}\right\} \tag{2.4}$$

Combining equations (2.2) and (2.3) we arrive at Wagner's equation

$$f(x, y) = h(t_c(x, y)) + \int_0^{t_c(x,y)} \phi_{,z}(x, y, 0, \tau)\, \mathrm{d}\tau. \tag{2.5}$$

Within the classical Wagner problem the body shape function $f(x, y)$ and the body velocity $U(t)$ are given and one needs to determine both the velocity potential

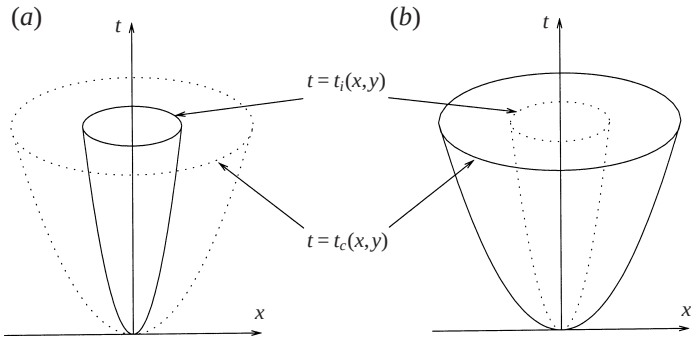

FIGURE 3. Illustration of (*a*) the direct and (*b*) the inverse problems; the dotted lines denote the surfaces which have to be determined; the outer and inner surfaces contain all the curves $\Gamma(t)$ and $\gamma(t)$, respectively.

$\phi(x, y, z, \tau)$, $0 < \tau < t_c(x, y)$, and the function $t_c(x, y)$ which satisfy equations (2.4) and (2.5). This problem is referred to as the direct problem. It is a very complicated one and the difficulties were emphasized in the introduction.

The inverse problem offers an attractive alternative to solve equation (2.5). In this problem the body velocity and the contact region shape are prescribed at any instant and it is necessary to determine the liquid flow and to reconstruct the entering body shape. This implies that the functions $U(t)$ and $t_c(x, y)$ are given and equation (2.5) yields the explicit expression for the shape function $f(x, y)$ provided the mixed boundary-value problem (2.4) has been solved.

In order to illustrate the difference between the direct and inverse Wagner problems, we consider the intersection line $\gamma(t)$ between the surface of the moving body $z = f(x, y) - h(t)$ and the initial liquid level $z = 0$. The intersection line is described by the equation $f(x, y) = h(t)$. It is convenient to introduce the new function $t_i(x, y)$ such that $h(t_i(x, y)) \equiv f(x, y)$ and $t_i(0, 0) = 0$. Equation $t_i(x, y) = t$ determines the three-dimensional surface in the space with coordinates x, y and t, a cross-section $t = \tau$ of which provides the intersection line $\gamma(\tau)$ at the time instant τ. It is clear that the surface $t = t_i(x, y)$ is located inside the surface $t = t_c(x, y)$, which is due to the piled-up effect (figure 3). Within the direct problem the surface $t = t_i(x, y)$ is given and one has to determine the surface $t = t_c(x, y)$, cross-sections of which provide the contact lines. Within the inverse problem the surface $t = t_c(x, y)$ is prescribed and one has to reconstruct the surface $t = t_i(x, y)$. Once the function $t_i(x, y)$ has been obtained, the body shape function is given as $f(x, y) = h(t_i(x, y))$ provided the penetration depth h is prescribed at any time instant.

It should be noted that the formulation of the inverse Wagner problem described above is possible because the liquid flow depends on the contact region shape $\mathscr{D}(\tau)$ and the body velocity $U(\tau)$ (see equations (2.4)) but not on the body shape. The inverse problem of impact is linear and, even in the most complicated cases, can be reduced to an integral equation with respect to the velocity potential $\phi(x, y, 0, \tau)$ on the disk $\mathscr{D}(\tau)$ and quadratures. It was proved by Zaremba (1910) that in the case of a continuously differentiable boundary of the region $\mathscr{D}(\tau)$ the solution of the mixed boundary-value problem (2.4) exists, is unique and continuous up to the boundary $z = 0$. Therefore, the solution of the inverse Wagner problem exists and is unique for smooth contact lines $\Gamma(\tau)$.

A common difficulty of both the inverse and direct problems is connected with calculation of the vertical velocity on the free surface $\phi_{,z}(x, y, 0, \tau)$ which appears

in the integrand of equation (2.5). An advantage of the inverse problem is that the corresponding velocity potential has now to be calculated for a flow around a flat disk bounded by a known curve $\Gamma(\tau)$. This can be done either numerically in the general case or analytically for simple curves $\Gamma(\tau)$. The former case is not considered here but a general method of solution is outlined in the next section. The latter case offers a wide range of exact solutions, which are detailed in §§ 4 and 5.

3. Method of solution

For a given curve $\Gamma(\tau)$ bounding the wetted area $\mathscr{D}(\tau)$, the inverse problem requires the calculation of the vertical velocity on the free surface. It is then introduced into the integrand of equation (2.5). The vertical velocity of the liquid free surface can be obtained from the representation of the velocity potential in the lower half-space, $z < 0$,

$$\phi(x,y,z,\tau) = -\frac{z}{2\pi}\iint_{\mathscr{D}(\tau)} \frac{\phi(\xi,\eta,0,\tau)\,\mathrm{d}\xi\mathrm{d}\eta}{((x-\xi)^2+(y-\eta)^2+z^2)^{3/2}}, \tag{3.1}$$

in the form

$$\phi_{,z}(x,y,0,\tau) = -\frac{1}{2\pi}\iint_{\mathscr{D}(\tau)} \frac{\phi(\xi,\eta,0,\tau)\,\mathrm{d}\xi\mathrm{d}\eta}{((x-\xi)^2+(y-\eta)^2)^{3/2}}, \tag{3.2}$$

where $(x,y) \in \mathscr{FS}(\tau)$. It was taken into account in (3.1) that $\phi(x,y,0,\tau) \equiv 0$ outside the contact region $\mathscr{D}(\tau)$. Once the contact region $\mathscr{D}(\tau)$ and the potential distribution $\phi(x,y,0,\tau)$ on it are known, formula (3.2) can be substituted into Wagner's condition (2.5) to provide the corresponding shape of the entering body. Special care has to be taken over the integration in (2.5) as the integration variable τ approaches the upper limit $t_c(x,y)$, which is due to the singularity of the vertical velocity $\phi_{,z}(x,y,0,\tau)$ at the contact line $\Gamma(\tau)$ (see Howison *et al.* 1991).

In order to calculate the potential $\phi(x,y,0,\tau)$ on the contact region $\mathscr{D}(\tau)$, we differentiate (3.1) with respect to z and consider the limit of the result as $z \to -0$. Taking the boundary condition on the wetted part of the body surface into account, one obtains the integral equation

$$-U(\tau) = \frac{1}{2\pi}\lim_{z\to-0}\frac{\partial^2}{\partial z^2}\iint_{\mathscr{D}(\tau)} \frac{\phi(\xi,\eta,0,\tau)\,\mathrm{d}\xi\mathrm{d}\eta}{\sqrt{(x-\xi)^2+(y-\eta)^2+z^2}}, \tag{3.3}$$

which has to be satisfied at any point (x,y) from $\mathscr{D}(\tau)$. The solution of equation (3.3) also has to satisfy the boundary condition: $\phi(x,y,0,\tau) = 0$ on the boundary $\partial\mathscr{D}(t)$ of the region $\mathscr{D}(\tau)$. In order to understand the necessity of the boundary condition for equation (3.3), we use the well-known formula

$$\frac{\partial^2}{\partial z^2}\left(\frac{1}{\sqrt{(x-\xi)^2+(y-\eta)^2+z^2}}\right) = -4\pi\delta(x-\xi)\delta(y-\eta)\delta(z) - \Delta_2\left(\frac{1}{\sqrt{(x-\xi)^2+(y-\eta)^2+z^2}}\right), \tag{3.4}$$

where $\delta(x)$ is the Dirac delta function and $\Delta_2 = \partial^2/\partial x^2 + \partial^2/\partial y^2$ is the two-dimensional Laplace operator. Substituting this formula into (3.3) and letting $z \to -0$, we obtain

the equation

$$\Delta_2 \iint_{\mathscr{D}(\tau)} \frac{\phi(\xi,\eta,0,\tau)\,\mathrm{d}\xi\mathrm{d}\eta}{\sqrt{(x-\xi)^2+(y-\eta)^2}} = 2\pi U(\tau), \quad (x,y)\in\mathscr{D}(\tau), \tag{3.5}$$

which is reminiscent of Poisson's equation. Solution of equation (3.5) with the boundary condition $\phi = 0$ on $\partial\mathscr{D}(\tau)$ can be obtained in the same way as that of (3.3).

The integral equation (3.3) was solved by Meyerhoff (1970) in the case of rectangular region $\mathscr{D}$ with the help of a double series similar to that used in lifting-surface theory. Basic functions which are combinations of the Chebyshev polynomial of the second kind, were adapted from those used by Glauert (1983) in the two-dimensional wing problem. Agreement of the numerical results for rigid plates with experimental data by Pabst (1930) is fairly good.

The three-dimensional problem of an elastic rectangular plate impact onto the liquid surface was analysed by Korobkin (1996). The problem requires the solution of equation (3.5), where the right-hand side is now a function of x, y, and τ and represents the local velocity of the elastic plate.

Equation (3.3) was rewritten by Watanabe (1986*a*, *b*, 1987) in the form

$$2\pi U(\tau) = \iint_{\mathscr{D}(\tau)} \frac{\phi(\xi,\eta,0,\tau)-\phi(x,y,0,\tau)}{((x-\xi)^2+(y-\eta)^2)^{3/2}}\mathrm{d}\xi\mathrm{d}\eta + \phi(x,y,0,\tau)\lim_{z\to 0}\iint_{\mathscr{D}(\tau)} \frac{\mathrm{d}\xi\mathrm{d}\eta}{((x-\xi)^2+(y-\eta)^2+z^2)^{3/2}}, \tag{3.6}$$

and solved numerically by a method similar to that of Meyerhoff (1970) but with different basic functions. Numerical calculations were performed for real ship hulls and the results obtained were compared with experiments.

The integral equation (3.3) was used by Takagi (1997) for the displacement potential, which is the integral in time of the velocity potential. An advantage of working with the displacement potential instead of the velocity potential is that the gradient of the displacement potential is zero together with the potential itself along the contact line $\Gamma(\tau) = \partial\mathscr{D}(\tau)$.

After some manipulations accounting for the boundary condition $\phi = 0$ on $\partial\mathscr{D}(\tau)$ equation (3.3) can be transformed to

$$\frac{\partial}{\partial y}\iint_{\mathscr{D}(\tau)} \frac{\partial\phi}{\partial\xi}(\xi,\eta,0,\tau)\frac{\sqrt{(x-\xi)^2+(y-\eta)^2}}{(x-\xi)(y-\eta)}\,\mathrm{d}\xi\mathrm{d}\eta = -2\pi U(\tau), \tag{3.7}$$

which is the well-known integral equation of wing theory (see, for example, Bisplinghoff, Ashley & Halfman 1996), or

$$\iint_{\mathscr{D}(\tau)} \frac{\partial\phi}{\partial\xi}(\xi,\eta,0,\tau)\frac{1}{(y-\eta)^2}\left[1+\frac{x-\xi}{\sqrt{(x-\xi)^2+(y-\eta)^2}}\right]\mathrm{d}\xi\mathrm{d}\eta = 2\pi U(\tau), \tag{3.8}$$

which was accurately solved by Tuck (1993). Equation (3.8) was solved for a rectangular region $\mathscr{D}$ of arbitrary aspect ratio with up to seven-digit accuracy. An explicit solution of equation (3.8) has been obtained for an elliptic region $\mathscr{D}$ by Hauptmann & Miloh (1986).

A finite element method was used by Donguy *et al.* (2000) to solve the three-dimensional impact problem with respect to the displacement potential. Calculations were performed for an axisymmetric cone.

We may conclude that the velocity potential distribution on the wetted area $\mathscr{D}(\tau)$

can be obtained numerically by solving one of the integral equations (3.3)–(3.8) which are similar to those well-known in wing theory. The solutions of these equations were obtained mainly for rectangular regions. Once the velocity potential is known, the vertical velocity on the free surface can be evaluated from equation (3.2). In order to perform accurate calculations, the velocity potential on the wetted area $\mathscr{D}(\tau)$ has to be evaluated with good accuracy. This is still not a simple task even if the numerical methods described in this section provide the global characteristics such as added mass with very good precision. Moreover, the boundary conditions in the impact problem and those in the lifting surface problem are not identical. In particular, the latter includes the Kutta conditions which are not considered in the problem of blunt-body impact. This means that the methods developed in wing theory must be used for the impact problem with special care. Accurate evaluation of the velocity potential on the contact region $\mathscr{D}(t)$ of an arbitrary shape is a subject of our further research.

There is a way to derive exact solutions of the inverse Wagner problem, thus providing preliminary qualitative results. These solutions are also helpful to test numerical solutions obtained for both the direct and inverse impact problem. Exact solutions can be obtained, in particular, for elliptic contact regions. For various applications of industrial interest the elliptic contact regions are general enough to cover a wide range of physical configurations. Korobkin (1985) found that the leading term in the asymptotic solution of the smooth- and blunt-body entry problem as $t \to 0$ is the same as if the entering body were an elliptic paraboloid. In addition the study of elliptic shapes also takes into account all kinds of axisymmetric bodies. The impact problem for elliptic disks has already been studied in previous works by Borodich (1988), Toyama (1996) and Wood (1997) among others.

In the following developments the elliptical case is fully analysed. The potential flow around an elliptic disk is given analytically as a degenerate case of the three-dimensional ellipsoid. We prescribe the two semi-axes of the contact line $\Gamma(t)$ as functions of time. This leads to the following alternative: these two semi-axes evolve dependently or not, in other words, the contact region grows homothetically or not. The latter problem can only be handled numerically but with a prescribed accuracy. The former case yields, among others, self-similar solutions. Exact solutions are presented when the two semi-axes of the elliptic region grow either as square root of time or linearly with time.

4. Impact problem for elliptic contact region

In this section the Wagner problem (2.4) and (2.5) is considered for elliptic contact region $\mathscr{D}(t)$. The position of the contact line $\Gamma(t)$ at an instant t is described by the equation

$$\frac{x^2}{a^2(t)} + \frac{y^2}{b^2(t)} = 1, \tag{4.1}$$

where the semi-axes $a(t)$ and $b(t)$ are given within the inverse impact problem and are the principal unknowns within the direct problem of impact (figure 4). The semi-axes are such that $b(t) \geqslant a(t)$ and $a(0) = b(0) = 0$. According to the main assumption of the Wagner theory the inequalities $a(t) \gg h(t)$ and $b(t) \gg h(t)$ have to be satisfied during the stage under consideration, $0 < t < t_1$. The impact problem with an elliptic contact region is a natural generalization of the axisymmetric impact problem, where $a(t) = b(t)$. It is convenient to introduce the aspect-ratio factor $k(t) = a(t)/b(t)$ and the

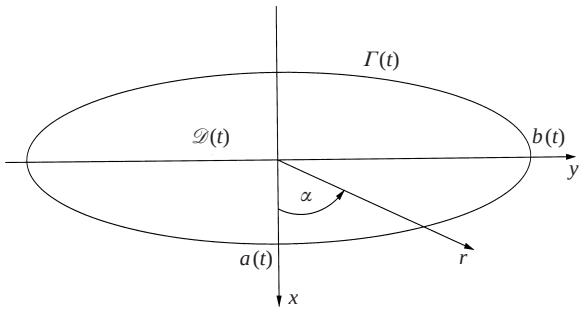

FIGURE 4. Elliptic contact region $\mathscr{D}(t)$ with the semi-axes $a(t)$ and $b(t)$ in the x- and y-directions, respectively. The angle α is measured from the positive x-axis.

ellipse eccentricity $e(t) = \sqrt{1 - k^2(t)}$. In the axisymmetric case $k(t) \equiv 1$ and $e(t) \equiv 0$. We say that the contact region expands homothetically if the aspect-ratio factor k is independent of time.

In the elliptic case the mixed boundary-value problem (2.4) was reduced by Leonov (1940) to equation (3.5). It was observed that the left-hand side of this equation does not depend on the spatial variables x and y if the following form of the solution is chosen:

$$\phi(x, y, 0, t) = S(t)\sqrt{1 - \frac{x^2}{a^2(t)} - \frac{y^2}{b^2(t)}}. \tag{4.2}$$

The function $S(t)$ is determined by substitution of (4.2) into equation (3.5). In order to evaluate the integral in (3.5), ellipsoidal coordinates (Appell 1932) have been used. Solution (4.2) satisfies the boundary condition $\phi = 0$ on $\Gamma(t)$. Leonov's solution was used by Borodich (1988) to obtain the vertical velocity of the free surface outside the elliptic disk and to derive equation (2.5) in the homothetical case.

The impact of an elliptic plate on a water surface was studied by Wood (1997) within the pressure-impulse theory. The pressure impulse on the plate was found in the form (4.2). Numerical calculations were performed for the pressure-impulse distribution throughout the liquid volume.

The easiest way to present the solution of the mixed boundary-value problem (2.4) in the elliptic case is to treat it as the limiting case of a vertically moving ellipsoid in an unbounded fluid. The time t is the parameter in (2.4), which is why we do not mention the dependence of the solution on time in treatment of (2.4). The solution of the impact problem for the elliptic disk is briefly derived below.

A rigid ellipsoid bounded by the surface

$$\frac{x^2}{a^2} + \frac{y^2}{b^2} + \frac{z^2}{c^2} = 1 \tag{4.3}$$

is considered. The elliptic disk (4.1) is the limit of this surface as $c \to 0$. Therefore, in our case $b \geqslant a > c$. The ellipsoidal coordinates λ, μ and ν are introduced as roots of the cubic equation

$$\frac{x^2}{a^2 + \theta} + \frac{y^2}{b^2 + \theta} + \frac{z^2}{c^2 + \theta} = 1 \tag{4.4}$$

with respect to θ, where $-b^2 < \nu < -a^2 < \mu < -c^2 < \lambda$. Surface (4.3) is described in the new coordinates by the equation $\lambda = 0$, which is easy to understand from equation (4.4). In the region outside the ellipsoid, we have $\lambda > 0$. The velocity potential $\varphi(x, y, z)$

of the unbounded liquid flow due to motion of the ellipsoid vertically downward with velocity U is given as (see Milne-Thomson 1960)

$$\varphi(x,y,z) = Cz \int_\lambda^\infty \frac{\mathrm{d}\xi}{(c^2+\xi)^{3/2}\sqrt{(a^2+\xi)(b^2+\xi)}}, \tag{4.5}$$

where $\lambda = \lambda(x,y,z)$ and, in particular,

$$z = -\sqrt{\frac{(c^2+\lambda)(c^2+\mu)(c^2+\nu)}{(a^2-c^2)(b^2-c^2)}}. \tag{4.6}$$

The constant C in (4.5) is determined from the boundary condition

$$\frac{\partial\varphi}{\partial n} = -U\cos\theta_z \quad (\lambda = 0) \tag{4.7}$$

on the surface (4.3), where θ_z is the angle between the normal to the surface of ellipsoid (4.3) and the z-axis. The limit of the potential $\varphi(x,y,z)$ as $c \to 0$ provides the solution of the boundary-value problem (2.4). The limit analysis has to be carried out carefully because some difficulties occur when both c and λ tend to zero in (4.5). Details of the limit analysis are given in Appendix A. As a result, the solution of the boundary-value problem (2.4) is obtained in the form

$$\phi(x,y,z) = \frac{Ua^2bz}{2E(e)} \int_{\lambda(x,y,z)}^\infty \frac{\mathrm{d}\xi}{\xi^{3/2}g(\xi)}, \tag{4.8}$$

where $g(\xi) = \sqrt{(a^2+\xi)(b^2+\xi)}$, $E(e) = E(\pi/2, e)$ and $\lambda(x,y,z)$ is the positive solution of equation (4.4) for $c = 0$. The standard elliptic function $E(N,e)$ is defined as

$$E(N,e) = \int_0^N \sqrt{1-e^2\sin^2\theta}\,\mathrm{d}\theta. \tag{4.9}$$

It should be noted that the elliptic disk (4.1) corresponds to $\lambda(x,y,0) = 0$. The integral in (4.8) is singular as $\lambda \to 0$. In order to obtain the velocity potential on the disk, we integrate by parts in equation (4.8) and consider the limit as $\lambda \to +0$ and $z \to -0$. The result is

$$\phi(x,y,0) = -\frac{Ua}{E(e)}\sqrt{1-\frac{x^2}{a^2}-\frac{y^2}{b^2}} \tag{4.10}$$

on the elliptic disk, where $x^2/a^2 + y^2/b^2 \leqslant 1$ (Scolan 1999). This exact result was compared to the approximate one by Toyama (1996), which is presented as a polynomial of fourth order with respect to the aspect-ratio factor k. The maximum relative error was found to be about 0.25% at $k \approx 0.714$.

In the axisymmetric case, $k = 1$, $e = 0$ and $E(0) = \pi/2$, the velocity potential (4.10) on the circular disk is $\phi(x,y,0) = -(2/\pi)U\sqrt{a^2-r^2}$, where $r^2 = x^2+y^2$, and coincides with that by Schmieden (1953). In the plane case, where $b/a \to \infty, e \to 1$ and $y = O(1)$, equation (4.10) provides $\phi(x,y,0) = -U\sqrt{a^2-x^2}$, which coincides with the result by Wagner (1932).

In the blunt-body impact problem the pressure in the liquid is given by the linearized Bernoulli equation $p(x,y,z,t) = -\rho\phi_{,t}(x,y,z,t)$. The hydrodynamic force $F(t)$ on the entering body follows from the pressure integration over the wetted area $\mathscr{D}(t)$:

$$F(t) = -\rho\iint_{\mathscr{D}(t)} \frac{\partial\phi}{\partial t}(x,y,0,t)\,\mathrm{d}x\,\mathrm{d}y = -\rho\frac{\mathrm{d}}{\mathrm{d}t}\iint_{\mathscr{D}(t)} \phi(x,y,0,t)\,\mathrm{d}x\,\mathrm{d}y. \tag{4.11}$$

Substituting (4.10) into the last integral and evaluating it, one finds

$$F(t) = \frac{\mathrm{d}}{\mathrm{d}t}[M_a(t)U(t)], \tag{4.12}$$

where $M_a(t)$ is the added mass of the elliptic disk (4.1):

$$M_a(t) = \frac{2\pi}{3}\frac{\rho a^2 b}{E(e)}. \tag{4.13}$$

It is seen that $M_a(0) = 0$ and $M_a = \frac{4}{3}\rho a^3$ in the axisymmetric case (Lamb 1932), where $a = b$.

The kinetic energy $T(t)$ of the liquid flow generated by the impact,

$$T(t) = \tfrac{1}{2}\rho \iint_{\mathscr{D}(t)} \phi(x, y, 0, t)\phi_{,z}(x, y, 0, t)\,\mathrm{d}x\,\mathrm{d}y = \tfrac{1}{2}M_a(t)U^2(t) \tag{4.14}$$

and the work $A(t)$ done to oppose the hydrodynamic force on the entering blunt body,

$$A(t) = \int_0^t F(\tau)U(\tau)\,\mathrm{d}\tau, \tag{4.15}$$

in general are not equal to each other. In the case of constant entry velocity equations (4.14) and (4.15) give $T(t) = \frac{1}{2}M_a(t)U^2$ and $A(t) = M_a(t)U^2$, respectively. This implies that the energy conservation law is not satisfied within the Wagner theory. In the general case,

$$\frac{\mathrm{d}}{\mathrm{d}t}[A(t) - T(t)] = \tfrac{1}{2}U^2\frac{\mathrm{d}M_a}{\mathrm{d}t}, \tag{4.16}$$

where $\mathrm{d}M_a/\mathrm{d}t > 0$ during the initial stage. It is seen, in particular, that $T(t) < A(t)$, which means that the energy is partly 'lost' during the impact.

This fact is well-known for both plane and axisymmetric cases (Korobkin 1994 and Molin, Cointe & Fontaine 1996). We know that the energy is partly transmitted to the main liquid body and partly to the spray jet. The latter part of the energy can be calculated by evaluating the jet velocity and its thickness. The flow in the jet root can be approximately considered as two-dimensional because the variation of the flow in the normal direction to the smooth contact line $\Gamma(t)$ is greater during the initial stage than that in the tangential direction. This means that the Wagner solution for the two-dimensional jet root region can be used to obtain parameters of the three-dimensional jet sheet formed at the periphery of the contact region. In order to obtain the uniformly valid solution, we need to isolate an elementary slice defined in the normal direction of $\Gamma(t)$ and to match there the three-dimensional outer solution (4.8) with the two-dimensional jet solution by Wagner (1932). The jet solution provides, in particular, that the maximum pressure $P_{max}(\alpha, t)$ in each elementary slice occurs in a close vicinity of the contact line and is equal to $\frac{1}{2}\rho V_n^2(\alpha, t)$, where $V_n(\alpha, t)$ is the normal component of the velocity of the expanding contact line. For an elliptic contact line (4.1), we obtain

$$V_n(\alpha, t) = \frac{a_{,t}\cos^2\alpha + kb_{,t}\sin^2\alpha}{\sqrt{1 - e^2\sin^2\alpha}}, \tag{4.17}$$

where $x = a(t)\cos\alpha$ and $y = b(t)\sin\alpha, 0 \leqslant \alpha < 2\pi$, along the line.

The total jet energy follows from the summation of the elementary contributions of each slice all over the contact line $\Gamma(t)$. This calculation seems only to be possible numerically for the most general case. However, one may expect that the result will

not be different from the two-dimensional one which stipulates that the kinetic energy is transferred equally to the jet and to the bulk of the fluid. In the three-dimensional case this proportion has to be checked numerically.

It should be noted that the evolution of the jet sheet is different from that of the two-dimensional jet and requires a special analysis. The evolution of the spray sheet in the axisymmetric case was studied by Korobkin (1997).

The vertical velocity $\phi_{,z}(x, y, z)$ of the liquid particles on the free surface, $z = 0$ and $x^2/a^2 + y^2/b^2 > 1$, follows from (4.8):

$$\frac{\partial \phi}{\partial z}(x, y, 0) = -\frac{U}{E(e)} \left[E\left(\arcsin \frac{b}{\sqrt{\lambda + b^2}}, e \right) - \sqrt{\frac{b^2(\lambda + a^2)}{\lambda(\lambda + b^2)}} \right], \tag{4.18}$$

where $\lambda = \lambda(x, y, t)$ is the positive root of equation (4.4) for $z = 0$:

$$\lambda = \tfrac{1}{2}[x^2 + y^2 - a^2 - b^2 + \sqrt{(eb)^4 + 2(eb)^2(x^2 - y^2) + (x^2 + y^2)^2}]. \tag{4.19}$$

Far from the contact region, $r \to \infty$, $z = 0$, where $r = \sqrt{x^2 + y^2}$, we obtain

$$\frac{\partial \phi}{\partial z} \sim \frac{U}{E(e)} \frac{a^2 b}{3} \frac{1}{r^3} + O(r^{-5}), \tag{4.20}$$

which is in agreement with the results by Schmieden (1953) in the axisymmetric case, $a = b$. We may conclude that far from the contact region the elevation of the free surface is approximately the same as in the axisymmetric problem with equivalent radius a_{eq} of the contact region being $(\pi a^2 b / 2E(e))^{1/3}$.

Formulae (4.18) and (4.19) make it possible to obtain the free surface elevation in quadratures by integrating (4.18) with respect to time for given functions $a(t)$, $b(t)$ and $U(t)$. Asymptotic formula (4.20) can be used instead of (4.18) to evaluate the vertical velocity far from the impact region.

5. Inverse Wagner problem for elliptic contact region

Within the inverse problem of impact we assume that the functions $a(t), b(t)$ and $U(t)$ are prescribed for $0 < t < t_1$. The functions are not arbitrary. They satisfy the following conditions: (i) $a(t)$, $b(t)$ and $U(t)$ belong to $C^1(0, t_1)$, (ii) $a(0) = 0, b(0) = 0$, (iii) $a(t)$ and $b(t)$ monotonically increase in the time interval $[0, t_1]$, (iv) $b(t) \geqslant a(t)$, (v) $U(t) > 0$, (vi) $\mathrm{d}a/\mathrm{d}t \gg U(t)$ and $\mathrm{d}b/\mathrm{d}t \gg U(t)$.

5.1. *General case of impact problem*

Taking into account the equality

$$h(t) = \int_0^t U(\tau)\, \mathrm{d}\tau, \tag{5.1}$$

formula (2.5) for the entering body shape can be rewritten as

$$f(x, y) = \int_0^{t_c(x,y)} [U(\tau) + \phi_{,z}(x, y, 0, \tau)]\, \mathrm{d}\tau, \tag{5.2}$$

where the function $t_c(x, y)$ is defined by equation (4.1) resolved with respect to t. In the polar coordinates r, α, where $x = r\cos\alpha$ and $y = r\sin\alpha$, equation (4.1) takes the form

$$r^2 \left[\frac{\cos^2\alpha}{a^2(t)} + \frac{\sin^2\alpha}{b^2(t)} \right] = 1 \tag{5.3}$$

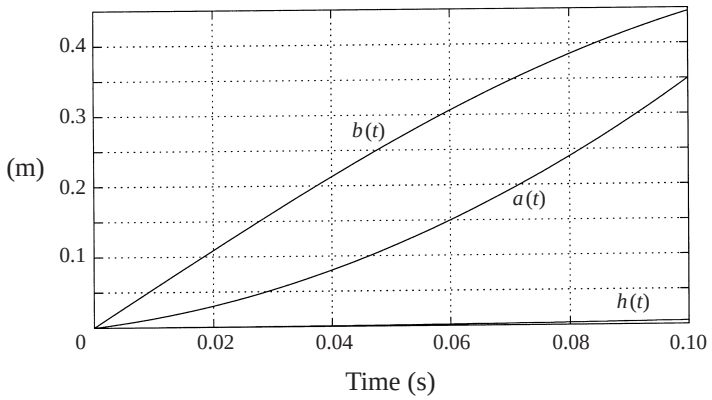

FIGURE 5. Time variation of the semi-axes $a(t)$ and $b(t)$, and penetration depth $h(t)$. The velocity is $U(t) = Gt$, the semi-axes are $a(t) = v_a t + \gamma_a t^2$ and $b(t) = x_b \sin \omega_b t$. The numerical parameters are $G = 1\,\mathrm{m\,s^{-2}}$, $v_a = 1\,\mathrm{m\,s^{-1}}$, $\gamma_a = 25\,\mathrm{m\,s^{-2}}$, $x_b = 0.5\,\mathrm{m}$ and $\omega_b = 7\pi/2\,\mathrm{s^{-1}}$. The simulation is performed until $t_1 = 0.1\,\mathrm{s}$.

and defines the function $t_c(r, \alpha)$. The properties (i)–(v) of the functions $a(t)$ and $b(t)$ make it possible to prove that $\partial t_c(r, \alpha)/\partial r > 0$, which implies that the inverse function $r = r(\alpha, t_c)$ such that $t_c[r(\alpha, t), \alpha] \equiv t$ can be introduced.

It is convenient to consider the main equation (5.2) in the parametric form. With the angular coordinate α and the upper limit t_c in (5.2) as parameters, $0 \leqslant \alpha < 2\pi$, $0 < t_c < t_1$, equations (5.2), (5.3), (4.19) and (4.18) yield

$$r = \frac{a(t_c)}{\sqrt{1 - e^2(t_c)\sin^2\alpha}}, \tag{5.4}$$

$$f(r, \alpha) = \int_0^{t_c} U(\tau)\left(1 + \frac{1}{E(e(\tau))}\left[\sqrt{\frac{\xi + k^2(\tau)}{\xi(\xi+1)}} - E\left(\arcsin\frac{1}{\sqrt{1+\xi}}, e(\tau)\right)\right]\right)\mathrm{d}\tau, \tag{5.5}$$

where $\xi = \lambda(r\cos\alpha, r\sin\alpha, \tau)/b^2(\tau)$,

$$\xi(r, \alpha, \tau) = \frac{1}{2}\left(\frac{r^2}{b^2(\tau)} - k^2(\tau) - 1 + \sqrt{\frac{r^4}{b^4(\tau)} + 2e^2(\tau)\frac{r^2}{b^2(\tau)}\cos 2\alpha + e^4(\tau)}\right). \tag{5.6}$$

The integrand in (5.5) vanishes as $\tau \to 0$, which follows from (4.20), and is singular at $\tau = t_c$, where $\xi(r, \alpha, t_c) = 0$. The singularity is integrable, which shows that numerical calculations of the body shape function $f(r, \alpha)$ can be performed with a given accuracy.

Numerical calculations were carried out with variables introduced as follows:

$$U(t) = Gt, \quad a(t) = v_a t + \gamma_a t^2, \quad b(t) = x_b \sin \omega_b t, \tag{5.7}$$

where G and γ_a have the same dimension as an acceleration, v_a is a velocity, x_b is a length and ω_b is a frequency. It should be noted that these developments are only used for small time t, when $a_{,t}(t) \gg U(t)$ and $b_{,t}(t) \gg U(t)$, in accordance with Wagner's assumptions. We choose $0 < t < t_1$, where $t_1 = 0.1\,\mathrm{s}$. As an example, the calculations are performed for the case

$$G = 1\,\mathrm{m\,s^{-2}}, \qquad \left.\begin{array}{ll} v_a = 1\,\mathrm{m\,s^{-1}}, & x_b = 0.5\,\mathrm{m}, \\ \gamma_a = 25\,\mathrm{m\,s^{-2}}, & \omega_b = 7\pi/2\,\mathrm{s^{-1}}, \end{array}\right\} \tag{5.8}$$

The time variation of the semi-axes $a(t)$ and $b(t)$ and the penetration depth $h(t)$ are shown in figure 5. Note that, according to the assumptions (i)–(vi) made at the

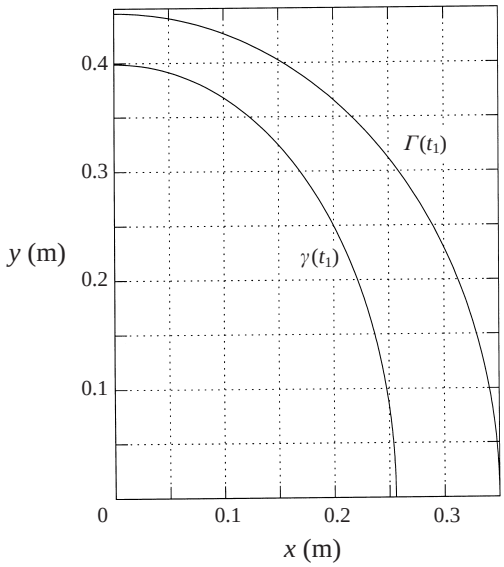

FIGURE 6. The contact line $\Gamma(t_1)$ and the intersection line $\gamma(t_1)$ at the instant t_1, $0 \leqslant \alpha \leqslant \pi/2$. Same parameters as in figure 5.

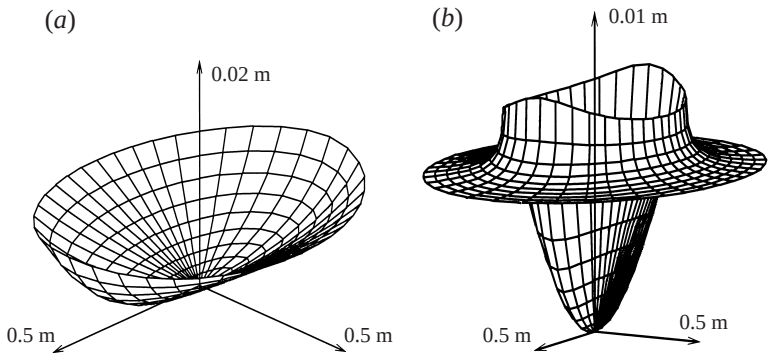

FIGURE 7. (*a*) Generated shape which provides the elliptic contact region with the semi-axes depicted in figure 5. The free surface elevation around the body shape is also drawn (*b*). The length scales are shown at the tip of arrows along the axes (x, y, z). Same parameters as in figure 5.

beginning of this section, the draught is always smaller that the two semi-axes. The relative positions of the intersection line $\gamma(t_1)$ and the contact line $\Gamma(t_1)$ at the end of the stage under consideration are shown in figure 6. Figure 7 shows perspectives of the generated shape of the body, the wetted part under the undisturbed free surface and the free surface elevation around the body. The corresponding distribution of maximum pressure $P_{max}(\alpha, t_1)$ along the contact line, $0 < \alpha < \pi/2$ is plotted in figure 8. It is seen that the pressure peaks at $\alpha = 0$, where the slope of the shape is lowest.

5.2. *Axisymmetric impact problem*

In the axisymmetric case the body shape function does not depend on the polar angle α and equations (5.4) and (5.5) provide

$$f(r) = \int_0^{t_c} U(\tau) \left[1 + \frac{2}{\pi} \left(\frac{a(\tau)}{\sqrt{r^2 - a^2(\tau)}} - \arcsin \frac{a(\tau)}{r} \right) \right] \mathrm{d}\tau, \quad r = a(t_c). \tag{5.9}$$

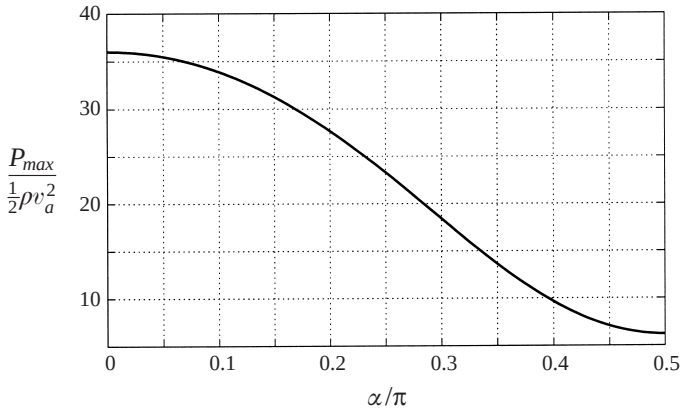

FIGURE 8. Distribution of the maximum pressure at the instant t_1 along the contact line, $0 < \alpha < \pi/2$. Same parameters as in figure 5.

This equation was derived and inverted with respect to $a(t)$ by Schmieden (1953).

Another way to invert this equation, to solve the direct problem in the axisymmetric case, is based on Wagner's method developed originally for the plane impact problem (Wagner 1932). After some manipulations equation (5.9) can be rewritten as

$$f(r) = \frac{2r}{\pi} \int_0^1 G(\xi r) \left(\arccos \xi + \frac{\xi}{\sqrt{1-\xi^2}} \right) \mathrm{d}\xi, \tag{5.10}$$

where $G(\xi r) = U(\tau)/a_{,\tau}(\tau)$ and τ is defined by the equation $a(\tau) = \xi r$ as the function of the product ξr. According to Wagner's method, the function $G(\xi r)$ is sought in the form

$$G(\xi r) = \sum_{n=0}^{\infty} G_n (\xi r)^n, \tag{5.11}$$

which gives

$$f(r) = \frac{2r}{\pi} \sum_{n=0}^{\infty} G_n r^{n+1} \int_0^1 \xi^n \left(\arccos \xi + \frac{\xi}{\sqrt{1-\xi^2}} \right) \mathrm{d}\xi. \tag{5.12}$$

This equation determines the coefficients G_n for a polynomial shape function $f(r)$. Taking into account the definition of the function $G(\xi r)$, we find $G(a(t)) = U(t)/a_{,t}(t)$, which leads to the following equation:

$$\sum_{n=0}^{\infty} \frac{G_n}{n+1} a^{n+1}(t) = h(t) \tag{5.13}$$

with respect to the radius $a(t)$ of the contact region. This equation can be solved either numerically or analytically for simple shape functions.

5.3. *Design of three-dimensional bodies entering water*

The semi-axes of the contact region $a(t)$ and $b(t)$ can be defined implicitly with the help of additional constraints, which can be viewed as the design problem (Scolan & Korobkin 2000). The design problem includes the solution of the inverse Wagner problem but can be much more complicated if the constraints are complex. We

consider the free fall of a blunt body onto an initially calm liquid free surface. The mass of the body M is given and the hydrodynamic force on the body $F(t) = F_*\beta(t/T)$, is prescribed for t being small enough. The contact region $\mathscr{D}(t)$ is assumed to be elliptic. We shall reconstruct the body shape, the entry of which provides the given resistance force. Here F_* is the constant, T is the time scale and $\beta(\tilde{t})$ is a non-dimensional function, $\tilde{t} = t/T$. The entering body shape has to be determined for given function $\beta(\tilde{t})$ and given constants U_0, F_*, T and e, where U_0 is the impact velocity. Two cases are considered: (i) $\beta(\tilde{t}) = 1$ and (ii) $\beta(\tilde{t}) = \tilde{t}\exp(-\tilde{t})$. The first is for the shape of a free falling body, for which the entry velocity reduces in an optimal way without high acceleration. The second case roughly imitates a typical history of the impact force.

The vertical velocity of the body $U(t)$ is governed by Newton's second law

$$MU_{,t} = Mg - F(t), \quad t > 0, \quad \text{and} \quad U(0) = U_0, \tag{5.14}$$

where g is the acceleration due to gravity and $F(t)$ is the hydrodynamic force acting on the entering body. Equations (5.14) and (4.12) give the body velocity as

$$U(t) = \frac{M(U_0 + gt)}{M + M_a(t)}. \tag{5.15}$$

Substitution of (5.15) into (4.12) yields the equation

$$F_*\beta(t/T) = \frac{\mathrm{d}}{\mathrm{d}t}\left[\frac{MM_a(t)(U_0 + gt)}{M + M_a(t)}\right], \tag{5.16}$$

integration of which in time provides the added mass $M_a(t)$:

$$M_a(t) = \frac{MF_*TB(t/T)}{M(U_0 + gt) - F_*TB(t/T)}, \quad B(\tilde{t}) = \int_0^{\tilde{t}} \beta(\tau)\,\mathrm{d}\tau. \tag{5.17}$$

Combining this equation with (4.13), we obtain the semi-axes $a(t)$ and $b(t)$ provided that the aspect-ratio factor $k(t)$ is specified from an additional condition. The simplest case, where $k = \sqrt{1 - e^2}$ is a constant, only is considered. With known semi-axes of the contact region, the inverse Wagner problem is solved according to the procedure described above.

In the first case the body acceleration is constant, $U(t) = U_0(1 - c_0t_1)$, and the semi-axes are

$$b(t) = b_0[t_1/(1 - c_0t_1)]^{1/3}, \quad a(t) = b(t)\sqrt{1 - e^2}, \tag{5.18}$$

$$t_1 = \frac{gt}{U_0}, \quad c_0 = \frac{F_*}{Mg} - 1, \quad b_0^3 = \left(\frac{3}{2\pi}\frac{E(e)}{1 - e^2}\right)\frac{F_*}{g\rho}. \tag{5.19}$$

It is seen that $b(t) = O(t^{1/3})$ as $t \to 0$, which indicates that $f(x, y) = O([x^2 + y^2]^{3/2})$ close to the impact point.

In the second case, $\beta(\tilde{t}) = \tilde{t}\exp(-\tilde{t})$, the semi-axes are given by the formulae

$$b(t) = b_0\delta^{1/3}\left[\frac{\gamma(t_1/\delta)}{1 + t_1 - \delta(c_0 + 1)\gamma(t_1/\delta)}\right]^{1/3}, \quad \delta = \frac{gT}{U_0}, \quad \gamma(\xi) = 1 - (1 + \xi)\exp(-\xi). \tag{5.20}$$

Now $f(x, y) = O([x^2 + y^2]^{3/4})$ close to the impact point.

Calculations were performed for the second case only with $U_0 = 4.43\,\mathrm{m\,s^{-1}}$, $F_* = 29333\,\mathrm{N}$, $T = 0.0113\,\mathrm{s}$ and $M = 100\,\mathrm{kg}$, which correspond to a falling height of 1 m and a maximum deceleration of $10g$. Two cases were considered: $e = 0.1$ and

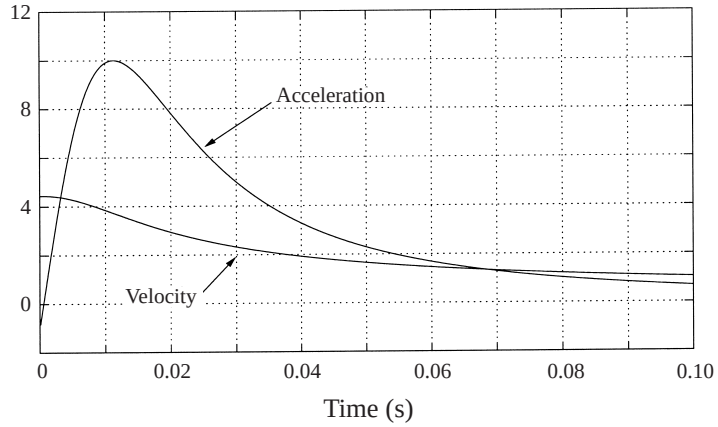

FIGURE 9. Non-dimensional velocity of the falling body $U(t)$ after the impact instant and the body acceleration $U_{,t}(t)$. The variables are made non-dimensioned with a unit velocity and gravity $g = 9.81\,\mathrm{m\ s^{-2}}$ respectively.

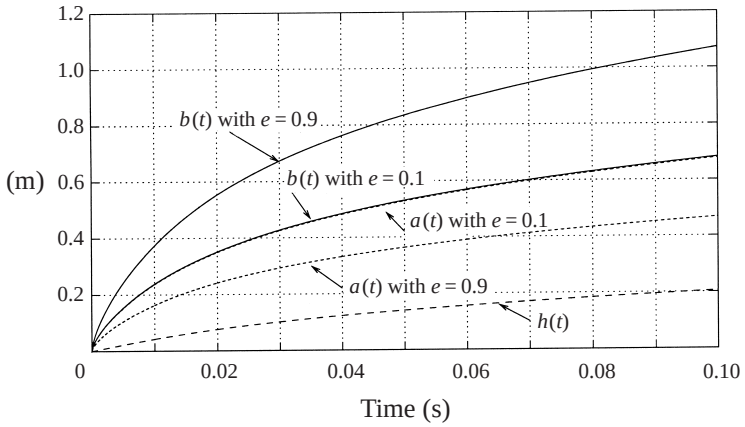

FIGURE 10. Time variation of semi-axes $a(t)$ and $b(t)$ for $e = 0.1$ and $e = 0.9$, and the body penetration depth $h(t)$.

$e = 0.9$. The time variations of the body acceleration and velocity are illustrated in figure 9. The time growths of the semi-axes $a(t)$ and $b(t)$ are depicted in figure 10. It should be noted that the penetration depth $h(t)$ is always smaller than the characteristic lengths of the contact region, which is in accordance with the hypothesis of linearization of Wagner's theory. The calculated body shapes and the free surface elevation around the bodies are plotted in figure 11. The calculated shapes can be used in drop experiments to justify the approach presented. The method described can be of help in designing bodies subject to water impact.

Both the axisymmetric problem and the design problem were considered for constant aspect-ratio factor k, which is the case of a homothetically expanding contact region. This case can be treated with the help of the general procedure based on equations (5.5). However, further simplifications are available and the radial dependence of the shape function $f(r, \alpha)$ can be better handled and even extracted if the velocity and the semi-axes are given as power functions of time.

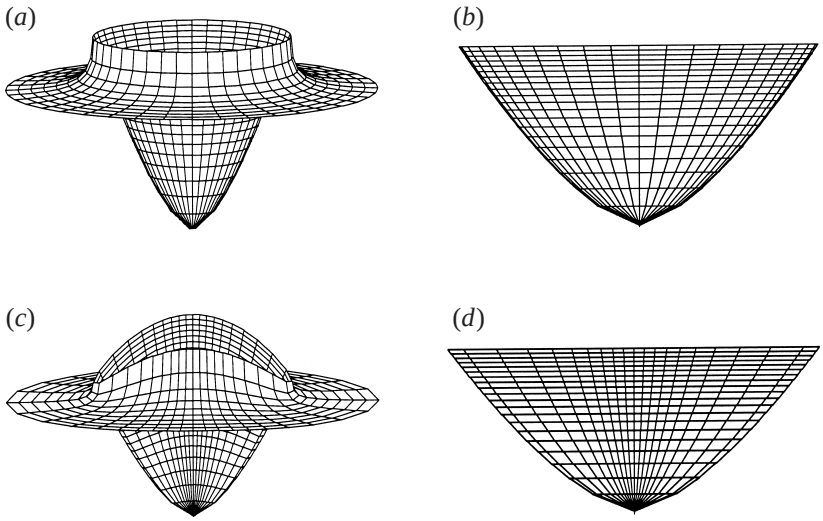

FIGURE 11. Calculated body shapes and free surface elevation around the designed bodies: eccentricity $e = 0.1$ in (a) and (b) and $e = 0.9$ in (c) and (d). Two successive contours along the body surface correspond to an interval of time 5×10^{-3} s. (a, c) Perspectives of the body with the successive contact lines on its surface; (b, d) projections on the plane $x = 0$ of the body shape under the undisturbed free surface. Shapes are drawn up to time $t = 0.1$ s; in (b) and (d) the ratio of maximum beam to penetration depth are $b/d \approx 5.5$ and $b/d \approx 9.6$ respectively.

5.4. *Homothetical case*

We start from equation (5.5), where the aspect-ratio factor k and the eccentricity e are the constants now. Taking into account that $\xi(r, \alpha, t_c) = 0$ and $h(0) = 0$, and integrating the right-hand side of equation (5.5) by parts, we obtain

$$f(r,\alpha) = \frac{1}{E(e)} \int_0^{t_c} \sqrt{\frac{\xi + k^2}{\xi(\xi+1)}} \left(U(\tau) - \frac{h(\tau)}{2(\xi+1)} \frac{\partial \xi}{\partial \tau}(r,\alpha,\tau) \right) \mathrm{d}\tau. \tag{5.21}$$

We suggest considering the quantity r in (5.21) as a function of the parameter t_c and the angular coordinate α, $r = r(t_c, \alpha)$. In the homothetical case

$$r(t_c,\alpha) = \frac{k}{\sqrt{1 - e^2 \sin^2 \alpha}} b(t_c), \tag{5.22}$$

which follows from (5.4). Equation (5.3) gives

$$b^2(\tau) = r^2(t_c,\alpha) \left[\frac{\cos^2 \alpha}{\xi + k^2} + \frac{\sin^2 \alpha}{\xi + 1} \right]. \tag{5.23}$$

The function $b(\tau)$ is monotonic, which makes it possible to invert (5.23) with respect to τ and consider equation (5.23) as the definition of a new function $\tau = \tau(q, r, \alpha)$, where $q = 1/\xi$. Taking q as the new integration variable, equation (5.21) can be transformed into

$$f(r,\alpha) = \frac{1}{E(e)} \int_0^{\infty} \left(U[\tau(q,r,\alpha)] \frac{\partial \tau}{\partial q} \sqrt{\frac{q(1+qk^2)}{1+q}} + \tfrac{1}{2} h[\tau(q,r,\alpha)] \sqrt{\frac{1+qk^2}{q(1+q)^3}} \right) \mathrm{d}q. \tag{5.24}$$

In formula (5.24), the radial coordinate r can be now considered as the independent variable, and the function $\tau(q, r, \alpha)$ is defined implicitly by the equation

$$b^2[\tau(q,r,\alpha)] = r^2 q \left[\frac{\cos^2\alpha}{1+qk^2} + \frac{\sin^2\alpha}{1+q}\right], \tag{5.25}$$

which follows from (5.23). In the most general case the integral in equation (5.24) can only be evaluated numerically. Equation (5.24) can be additionally simplified for $U(t)$ and $b(t)$ being power functions of time. This choice provides analytical solutions of the three-dimensional Wagner problem.

We consider the inverse Wagner problem in the case

$$U(t) = U_0 t^m, \quad b(t) = b_0 t^n, \tag{5.26}$$

where U_0 and b_0 are the given constants with proper dimensions, $m > -1$, $n > 0$ and $n \leqslant m + 1$. The last inequality follows from the original assumption $h(t) \ll b(t)$. Substituting (5.26) into (5.25), we obtain

$$\tau(q,r,\alpha) = r^{1/n} R(q,\alpha), \quad R(q,\alpha) = \frac{q^{1/2n}}{b_0^{1/n}} \left[\frac{\cos^2\alpha}{1+qk^2} + \frac{\sin^2\alpha}{1+q}\right]^{1/2n}. \tag{5.27}$$

Accounting for equations (5.26) and (5.27) formula (5.24) gives

$$f(r,\alpha) = r^{(m+1)/n} C(\alpha), \tag{5.28}$$

$$C(\alpha) = \frac{U_0}{E(e)} \int_0^\infty \left(R^m(q,\alpha) \frac{\partial R}{\partial q} \sqrt{\frac{q(1+qk^2)}{1+q}} + \frac{R^{m+1}(q,\alpha)}{2(m+1)} \sqrt{\frac{1+qk^2}{q(1+q)^3}} \right) \mathrm{d}q. \tag{5.29}$$

Therefore, in the case of (5.26) the dependence of the shape function $f(r, \alpha)$ on the radial coordinate r is simple and we need only to evaluate accurately the integral in (5.29).

The form of the shape function (5.28) in the homothetical case with power functions $U(t)$ and $b(t)$ was obtained by Borodich (1988). However, the coefficient $C(\alpha)$ was presented in another, more complicated form, which forced Borodich to conclude that there is no hope of evaluating $C(\alpha)$ analytically for any m and n.

6. Analytical solutions and their applications

Analytical solutions of the three-dimensional impact problem can be obtained, at least in the following three cases: (i) $m = 0$ and $n = \frac{1}{2}$; (ii) $m = 1$ and $n = 1$; (iii) $m = 0$ and $n = 1$. The first and second cases correspond to the impact problem for an elliptic paraboloid, and the third one to the impact problem for a cone.

6.1. *Entry of an elliptic paraboloid at a constant velocity*

In the case $m = 0$ and $n = \frac{1}{2}$, the body velocity is constant, $U(t) = U_0$, and the elliptic contact region expands homothetically, $a(t) = kb(t)$, with $b(t)$ increasing as the square root of time, $b(t) = b_0 t^{1/2}$. Equations (5.28) and (5.29) yield

$$f(r,\alpha) = r^2 C(\alpha), \tag{6.1}$$

$$C(\alpha) = \frac{U_0}{E(e)} \int_0^\infty \left(\frac{\partial R}{\partial q}(q,\alpha) \sqrt{\frac{q(1+qk^2)}{1+q}} + \tfrac{1}{2} R(q,\alpha) \sqrt{\frac{1+qk^2}{q(1+q)^3}} \right) \mathrm{d}q, \tag{6.2}$$

where

$$R(q,\alpha)=\frac{q}{b_0^2}\left[\frac{\cos^2\alpha}{1+qk^2}+\frac{\sin^2\alpha}{1+q}\right], \tag{6.3}$$

$$\frac{\partial R}{\partial q}(q,\alpha)=\frac{1}{b_0^2}\left[\frac{\cos^2\alpha}{(1+qk^2)^2}+\frac{\sin^2\alpha}{(1+q)^2}\right]. \tag{6.4}$$

It is easy to observe that

$$C(\alpha)=A_0\cos^2\alpha+B_0\sin^2\alpha, \tag{6.5}$$

where

$$A_0=\frac{U_0}{b_0^2E(e)}\left[\int_0^\infty q^{1/2}(1+q)^{-1/2}(1+qk^2)^{-3/2}\,\mathrm{d}q \right.$$
$$\left.+\frac{1}{2}\int_0^\infty q^{1/2}(1+q)^{-3/2}(1+qk^2)^{-1/2}\,\mathrm{d}q\right], \tag{6.6}$$

$$B_0=\frac{3U_0}{2b_0^2E(e)}\int_0^\infty q^{1/2}(1+q)^{-5/2}(1+qk^2)^{1/2}\mathrm{d}q. \tag{6.7}$$

The integrals in these equations are standard (see Gradshteyn & Ryzhik 1994), and give the following compact formulae:

$$A_0=\frac{U_0}{b_0^2k^2}\left[2-k^2\frac{D(e)}{E(e)}\right],\quad B_0=\frac{U_0}{b_0^2}\left[1+k^2\frac{D(e)}{E(e)}\right], \tag{6.8}$$

where $D(e)$ is the standard elliptic integral

$$D(e)=\frac{1}{e^2}[K(e)-E(e)],\quad K(e)=\int_0^{\pi/2}\frac{\mathrm{d}\theta}{\sqrt{1-e^2\sin^2\theta}}. \tag{6.9}$$

In the original Cartesian coordinates, $x=r\cos\theta$, $y=r\sin\theta$ and z, the equation obtained for the entering body shape function takes the form

$$f(x,y)=A_0x^2+B_0y^2, \tag{6.10}$$

which is the equation of an elliptic paraboloid. This result confirms the hypothesis by Korobkin (1985) that an elliptic paraboloid entering calm water at a constant velocity provides an elliptic contact region. The analytical solution obtained for the inverse Wagner problem can be used to derive the solution of the corresponding direct problem of water impact by an elliptic paraboloid.

The problem of an elliptic paraboloid entering initially calm liquid at a constant velocity is considered. The position of the moving body at time instant t is given by the equation

$$z=\frac{x^2}{A^2}+\frac{y^2}{B^2}-U_0t, \tag{6.11}$$

where A, B and U_0 are given constants and $B>A$. Equation (6.10) shows that within the Wagner approach the contact region $\mathscr{D}(t)$ of the entering body (6.11) with the liquid is a homothetically expanding ellipse with its semi-axes being $b(t)=b_0\sqrt{t}$ and $a(t)=b_0k\sqrt{t}$. The constants b_0 and k are unknown in advance and have to be determined for given A, B and U_0. In order to obtain the corresponding formulae, we compare equations (6.11) and (6.10) and conclude that the aspect-ratio factor k

of the contact region and the constant b_0 have to satisfy the following equalities:

$$A_0 = A^{-2}, \quad B_0 = B^{-2}, \tag{6.12}$$

where the functions $A_0(b_0, k)$ and $B_0(b_0, k)$ are defined in equations (6.8). Taking into account formulae (6.8) for A_0 and B_0, we obtain the equation for k:

$$k^2 \frac{1 + k^2 D(e)/E(e)}{2 - k^2 D(e)/E(e)} = k_\gamma^2, \tag{6.13}$$

where $k_\gamma = A/B$ is the aspect-ratio parameter which characterizes the slenderness of the body, and the formula for b_0 is

$$b_0 = B U_0^{1/2} \left[1 + k^2 \frac{D(e)}{E(e)}\right]^{1/2}. \tag{6.14}$$

Equations (6.13) and (6.14) together with (4.10) yield the solution of the impact problem for the elliptic paraboloid.

In order to compare this exact solution with the approximate one by Korobkin (1985), we consider the intersection line $\gamma(t)$ between the surface of the entering body (6.11) and the initial liquid level, $z = 0$ (see § 2). Equation (6.11) gives that this line is the ellipse with semi-axes $a_\gamma(t) = A\sqrt{U_0 t}$, $b_\gamma(t) = B\sqrt{U_0 t}$ and eccentricity $e_\gamma = \sqrt{1 - A^2/B^2}$. Korobkin (1985) obtained the following explicit formulae:

$$\frac{a_\gamma(t)}{a(t)} = \left[\frac{2 - e^2 - e_\gamma^2}{3(1 - e^2)}\right]^{1/2}, \tag{6.15}$$

$$e = e_\gamma \left[\frac{2 - e_\gamma^2}{3 - 2e_\gamma^2}\right]^{1/2}. \tag{6.16}$$

He worked with the displacement potential instead of the velocity potential and solved the corresponding boundary-value problem using Lamé functions. The solution was obtained in quadratures together with equation (6.15). However, it was not easy to satisfy the additional condition $\phi = 0$ on the contact line. This condition was satisfied approximately and equation (6.16) was derived from the analysis of the results of numerical calculations. The importance of the condition on the contact line has been discussed in § 3. The approximate solution by Korobkin (1985) can be improved, which will be shown in a subsequent paper by the authors devoted to the methods of solution of the direct three-dimensional Wagner problem. It should be noted that the approximate formula (6.16) provides the correct solutions (see Korobkin & Pukhnachov 1988) for the axisymmetric case, where $e_\gamma \to 0$, and for the plane case, where $e_\gamma \to 1$. Equation (6.13) can be rewritten in the form

$$e_\gamma^2 = 1 - (1 - e^2) \frac{1 + (1 - e^2) D(e)/E(e)}{2 - (1 - e^2) D(e)/E(e)}. \tag{6.17}$$

It can be proved that equation (6.15) is exact provided that e_γ is given by (6.17). Figure 12 shows the comparison between the exact solution (6.17) and the approximate one (6.16). The discrepancies are within 8%. It should be noted that the ratio e/e_γ is less than unity, which means that the elliptic contact region $\mathscr{D}(t)$ is less elongated than the elliptic cross-sections of the entering body. This is also confirmed by the results plotted in figure 13, where both the contact line $\Gamma(t)$ and the intersection line $\gamma(t)$ are shown at different time instants for a particular impact conditions $U_0 = 1\,\mathrm{m\,s^{-1}}$,

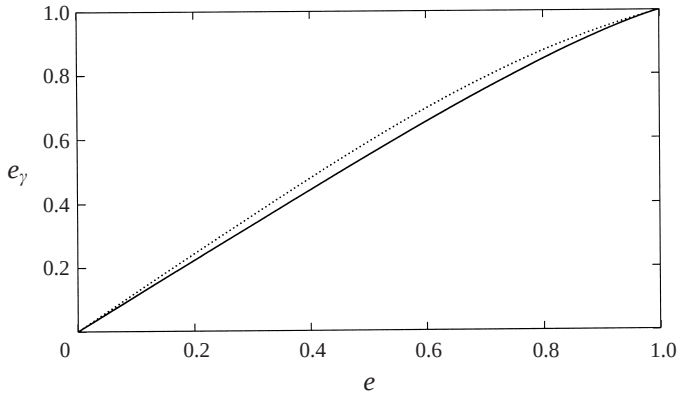

FIGURE 12. Graph of the eccentricity e_γ of the intersection line $\gamma(t)$ as a function of the eccentricity e of the contact line $\Gamma(t)$ for elliptic paraboloid entry problem: present exact solution (6.17) is shown with dotted line and the approximate solution (6.16) is shown with solid line.

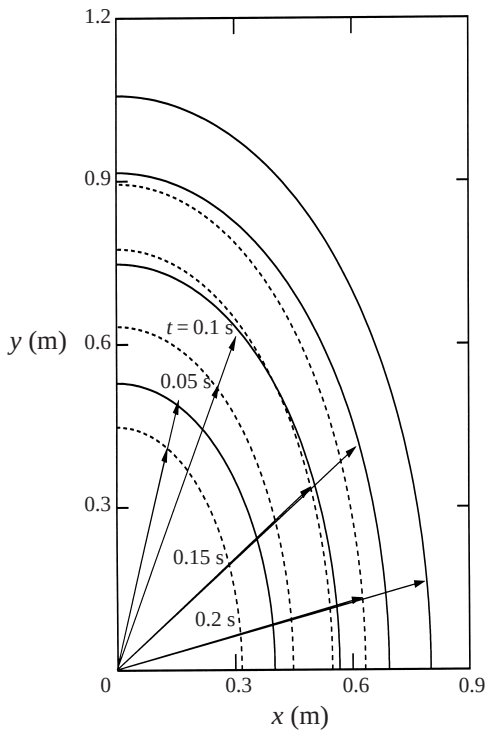

FIGURE 13. The contact lines $\Gamma(t)$ (solid curves) and intersection lines $\gamma(t)$ (dotted curves) at different time instants for $U_0 = 1\,\mathrm{m\,s^{-1}}$, $A_0 = A^{-2} = 0.5\,\mathrm{m^{-1}}$, $B_0 = B^{-2} = 0.25\,\mathrm{m^{-1}}$, simulation is performed in the time interval $t \in [0\,\mathrm{s}, 0.2\,\mathrm{s}]$.

$A_0 = A^{-2} = 0.5\,\mathrm{m^{-1}}$, $B_0 = B^{-2} = 0.25\,\mathrm{m^{-1}}$ and $0 < t < 0.2\,\mathrm{s}$. Figure 14 shows several intersection lines, $(x, y) \in \Gamma(t)$, $z = x^2/A^2 + y^2/B^2 - U_0 t$, between the entering elliptic paraboloid and the disturbed free surface. Note that the vertical dimension is magnified in this figure. It is seen that these lines are not two-dimensional curves, $x^2/A^2 + y^2/B^2 - U_0 t \neq \mathrm{Const}$ for $(x, y) \in \Gamma(t)$.

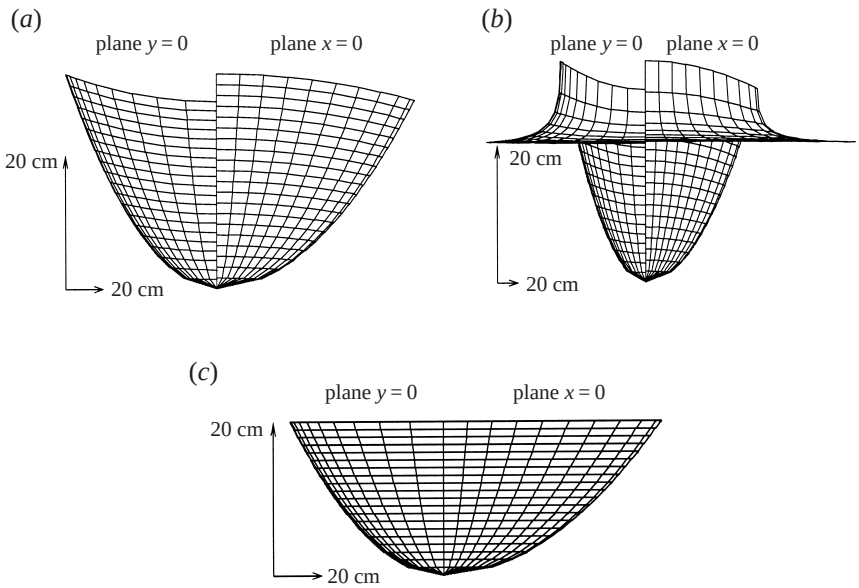

FIGURE 14. Elliptic paraboloid with $n = \frac{1}{2}$ and $m = 0$; projections onto the planes $y = 0$ and $x = 0$; see parameters in figure 13. (*a*) Elliptic paraboloid drawn with the successive contact lines on its surface; (*b*) similar to (*a*) but the free surface deformation is shown; (*c*) elliptic paraboloid with the successive intersection lines on its surface. Note the difference between the vertical and horizontal scales.

6.2. *Uniform acceleration of an elliptic paraboloid*

In the case $m = n = 1$, the body acceleration is constant, $U(t) = a_0 t$, and the elliptic contact region expands homothetically, $a(t) = kb(t)$, with $b(t)$ increasing linearly in time, $b(t) = b_0 t$. Equations (5.28) and (5.29) give

$$f(r, \alpha) = r^2 C(\alpha), \tag{6.18}$$

$$C(\alpha) = \frac{a_0}{2E(e)} \int_0^\infty \left(\frac{\partial R^2}{\partial q}(q, \alpha) \sqrt{\frac{q(1+qk^2)}{1+q}} + \tfrac{1}{2} R^2(q, \alpha) \sqrt{\frac{1+qk^2}{q(1+q)^3}} \right) \mathrm{d}q, \tag{6.19}$$

$$R^2(q, \alpha) = \frac{q}{b_0^2} \left[\frac{\cos^2 \alpha}{1+qk^2} + \frac{\sin^2 \alpha}{1+q} \right], \tag{6.20}$$

The formulae obtained coincide with those derived in § 6.1, which makes it possible to write down the final result for the shape function as

$$f(x, y) = A_1 x^2 + B_1 y^2, \tag{6.21}$$

where (see equations (6.5), (6.8) and (6.10))

$$A_1 = \frac{a_0}{2b_0^2 k^2} \left[2 - k^2 \frac{D(e)}{E(e)} \right], \quad B_1 = \frac{a_0}{2b_0^2} \left[1 + k^2 \frac{D(e)}{E(e)} \right]. \tag{6.22}$$

We may conclude now that any elliptic paraboloid entering water with uniform acceleration has an elliptic contact region which expands homothetically and linearly in time.

In order to solve the direct Wagner problem, we consider the equation for the position of the entering body in the form

$$z = \frac{x^2}{A^2} + \frac{y^2}{B^2} - \frac{a_0}{2}t^2. \tag{6.23}$$

Comparing equations (6.21) and (6.23), we conclude that equation (6.13) for the eccentricity e of the contact region is valid in the present case as well, and the quantity b_0 is given by

$$b_0 = B\left(\frac{a_0}{2}\right)^{1/2}\left[1 + k^2\frac{D(e)}{E(e)}\right]^{1/2}. \tag{6.24}$$

Equation (6.15) is also valid in the case under consideration.

6.3. *Impact of a cone*

In the case $m = 0$, $n = 1$, the entry velocity is constant, $U(t) = U_0$, and the body is pointed, $f(r, \alpha) = rC(\alpha)$, where the function $C(\alpha)$ is given by (5.29). The contact region is elliptic and expands homothetically, $a(t) = kb(t)$, where $b(t) = b_0 t$. For the pointed body

$$C(\alpha) = \frac{U_0}{E(e)}\int_0^\infty \left(\frac{\partial R}{\partial q}(q,\alpha)\sqrt{\frac{q(1+qk^2)}{1+q}} + \tfrac{1}{2}R(q,\alpha)\sqrt{\frac{1+qk^2}{q(1+q)^3}}\right)\mathrm{d}q, \tag{6.25}$$

$$R(q,\alpha) = \frac{\sqrt{q}}{b_0}\frac{\sqrt{1+qQ(\alpha)}}{\sqrt{(1+q)(1+qk^2)}}, \tag{6.26}$$

$$Q(\alpha) = \cos^2\alpha + k^2\sin^2\alpha, \tag{6.27}$$

where the integral can be expressed with the help of elementary functions. However, the calculations are not as simple as before. We suggest returning to the general formula (5.29) and presenting it as follows:

$$C(\alpha, e) = \frac{U_0 k}{2nE(e)}\left(\frac{Q(\alpha)}{b_0^2k^2}\right)^d\left[\frac{1}{2d}N(0,1,1) + A(\alpha)N(0,2,0) + B(\alpha)N(2,0,0)\right], \tag{6.28}$$

$$N(\lambda,\mu,\gamma) = \int_0^\infty \frac{q^{d-1/2}(q+Q^{-1}(\alpha))^{d+\gamma-1}\mathrm{d}q}{(q+1)^{d+3/2-\lambda}(q+k^{-2})^{d+1/2-\mu}}, \tag{6.29}$$

$$A(\alpha) = \frac{k^2\sin^2\alpha}{Q(\alpha)}, \qquad B(\alpha) = \frac{\cos^2\alpha}{k^2Q(\alpha)}, \qquad d = \frac{m+1}{2n}. \tag{6.30}$$

In the case under consideration, $m = 0$, $n = 1$ and $d = \frac{1}{2}$, integrals (6.29) can be evaluated analytically and (6.28) gives

$$C(\alpha, e) = \frac{U_0}{2b_0E(e)}\left[S_1\cos^2\alpha + S_2\sin^2\alpha + S_3\right] \tag{6.31}$$

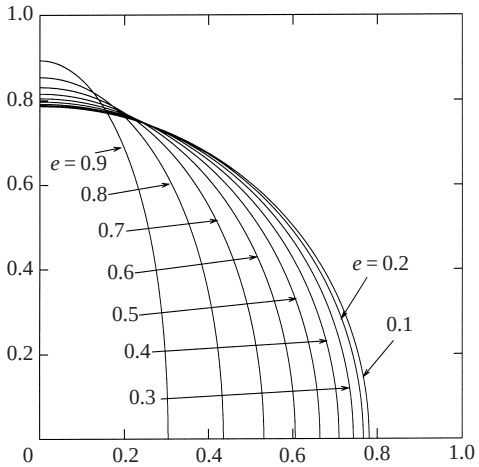

FIGURE 15. Cross-sections of the cone for different values of the parameter e, $0 < \alpha < \pi/2$.

with

$$\left.\begin{aligned} S_1 &= \int_0^\infty \frac{\mathrm{d}q}{(1+qk^2)\sqrt{1+qQ(\alpha)}} = \frac{2}{ke\cos\alpha}\arctan\frac{e\cos\alpha}{k}, \\ S_2 &= \int_0^\infty \frac{(1+qk^2)}{(1+q)^2\sqrt{1+qQ(\alpha)}}\mathrm{d}q \\ &= \frac{1}{\sin^2\alpha} + \left(\frac{1-(1+k^2)\sin^2\alpha}{2e\sin^3\alpha}\right)\ln\frac{1-e\sin\alpha}{1+e\sin\alpha}, \\ S_3 &= \int_0^\infty \frac{\sqrt{1+qQ(\alpha)}}{(1+q)^2}\mathrm{d}q = 1 + \frac{(e^2\sin^2\alpha-1)}{2e\sin\alpha}\ln\frac{1-e\sin\alpha}{1+e\sin\alpha}. \end{aligned}\right\} \tag{6.32}$$

In the axisymmetric case, $e = 0$, we obtain

$$C(\alpha, 0) = \frac{4}{\pi}\frac{U_0}{b_0}. \tag{6.33}$$

This result is in agreement with that of Shiffman & Spencer (1951), who studied the axisymmetric problem of cone entry.

In order to solve the corresponding direct problem of the impact, we introduce the function $C_0(\alpha, e) = (b_0/U_0)C(\alpha, e)$ and consider the entry problem for a pointed body, the position of which is described by the equation

$$z = A_2 C_0(\alpha, e)r - U_0 t. \tag{6.34}$$

Here U_0 is the body velocity, A_2 is a given constant which specifies the deadrise angle of the cone, and $C_0(\alpha, e)$ is the function defined above. Comparing (6.34) with the equation for the entering body shape, $f(r, \alpha) = C(\alpha)r$, obtained within the inverse Wagner problem, we conclude that the contact region in this case is elliptic with the semi-axes being $b(t) = U_0 t/A_2$ and $a(t) = U_0 kt/A_2$. Cross-sections of the body (6.34) by horizontal planes $z = z_0$, $z_0 > 0$, are described by the equation $r = z_0/(A_2 C_0(\alpha, e))$. Curves $r = 1/C_0(\alpha, e)$ are shown in figure 15 for different values of the parameter e.

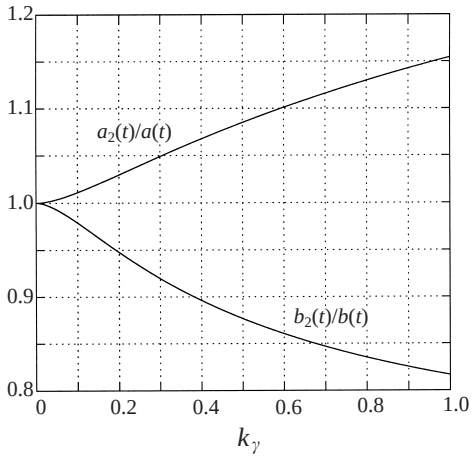

FIGURE 16. Ratios $a_{(2)}(t)/a(t)$ and $b_{(2)}(t)/b(t)$ as functions of the parameter $k_\gamma = A/B$: $a(t)$ and $b(t)$ are the semi-axes of the contact region $\mathscr{D}(t)$ predicted by Wagner theory; $a_{(2)}(t)$ and $b_{(2)}(t)$ are the semi-axes of the contact region $\mathscr{D}(t)$ given by the strip theory.

6.4. *Strip theory for elongated bodies*

In the case of elongated bodies, strip theory is frequently used to obtain approximate solutions of the three-dimensional impact problem. Within this theory the three-dimensional impact process is approximated by a sequence of two-dimensional impacts of each vertical cross section of the body. With the help of exact analytical solutions obtained for the three-dimensional impact problem we can check the applicability of the strip theory and give estimations of accuracy of approximate results.

The case of an elongated elliptic paraboloid is considered. The position of the body entering liquid at the constant velocity U_0 is described by equation (6.11), where $B \gg A$ now.

In the strip theory the body cross-sections $y = y_0$ are considered and the corresponding two-dimensional impact problems are formulated for each cross-section, the position of which is given as

$$z = \frac{1}{A^2}x^2 - U_0(t - t_0), \qquad t_0 = \frac{y_0^2}{U_0 B^2}. \tag{6.35}$$

The quantity t_0 indicates the time instant at which the cross-section $y = y_0$ reaches the undisturbed water surface. The solution of the plane problem of the parabolic contour entry was given by Wagner (1932). The half-width of the contact zone is $\bar{a}(t, y_0) = A\sqrt{2U_0(t - t_0)}$, $t > t_0$, the velocity potential in the contact zone is $\phi_{(2)}(x, y_0, 0, t) = -U_0\sqrt{\bar{a}^2(t, y_0) - x^2}$, $|x| < \bar{a}(t, y_0)$, and the elementary hydrodynamic force ΔF on the cross-section considered is given by

$$\Delta F = \frac{\mathrm{d}}{\mathrm{d}t}\left[\frac{\pi}{2}\rho\bar{a}^2(t, y_0)U_0\right]\Delta y_0, \tag{6.36}$$

where Δy_0 is the thickness of the cross-section slice.

The contact line $\Gamma_{(2)}(t)$ is given by the strip theory in the parametric form

$$y = y_0, \qquad x = \bar{a}(t, y_0), \tag{6.37}$$

which gives

$$\frac{x^2}{(A\sqrt{2U_0t})^2} + \frac{y^2}{(B\sqrt{U_0t})^2} = 1. \tag{6.38}$$

It is seen that the contact region within strip theory is the ellipse with the semi-axes $a_{(2)}(t) = A\sqrt{2U_0t}$ and $b_{(2)}(t) = B\sqrt{U_0t}$. The exact solution gives $a(t) = b_0k\sqrt{t}$ and $b(t) = b_0\sqrt{t}$, where k and b_0 are defined by equations (6.13) and (6.14). The ratios $a_{(2)}(t)/a(t)$ and $b_{(2)}(t)/b(t)$ are independent of time and are depicted in figure 16 as functions of the parameter $k_\gamma = A/B$. The following asymptotic formulae are valid as $k_\gamma \to 0$:

$$\frac{a_{(2)}(t)}{a(t)} = 1 - \tfrac{1}{8}k_\gamma^2 \ln k_\gamma + O(k_\gamma^2), \tag{6.39}$$

$$\frac{b_{(2)}(t)}{b(t)} = 1 + \tfrac{1}{2}k_\gamma^2 \ln k_\gamma + O(k_\gamma^2). \tag{6.40}$$

In order to derive these asymptotic formulae, equations (6.15) and (6.16) were used. Equation (6.16) is not exact but it approximates the more complicated equation (6.13) with good accuracy for $1 - e_\gamma^2 \ll 1$. Equations (6.39) and (6.40) show that strip theory overpredicts the length of the minor-axis of the contact region, $a(t)$, and underpredicts that of the major-axis, $b(t)$. The result (6.40) is unexpected because strip theory does not account for the piled-up effect at the line $x = 0$, which leads to the equality $b_{(2)}(t) = b_\gamma(t)$, where $b_\gamma(t)$ is the major semi-axis of the intersection curve $\gamma(t)$. Equation (6.40) indicates that for elongated bodies the ratio $(b(t) - b_\gamma(t))/b(t)$ is small. Strip theory determines the dimensions of the contact region with a relative error of less than 3% for an elliptic paraboloid with $A < B/10$.

Using the definitions of the functions $\bar{a}(t, y)$, $a_{(2)}(t)$ and $b_{(2)}(t)$, it is easy to check that $\bar{a}(t, y) = a_{(2)}(t)[1 - y^2b_{(2)}^{-2}(t)]^{1/2}$. With the help of this equality the distribution of the velocity potential over the contact region (6.38) can be presented within strip theory as

$$\phi_{(2)}(x, y, 0, t) = -U_0\sqrt{\bar{a}^2(t, y) - x^2} = -U_0a_{(2)}(t)\sqrt{1 - \frac{x^2}{a_{(2)}^2(t)} - \frac{y^2}{b_{(2)}^2(t)}}. \tag{6.41}$$

Taking into account that $E(e) \to 1$ as $e \to 1$ and comparing (6.41) with (4.10), we obtain

$$\phi_{(2)}(x, y, 0, t) \to \phi(x, y, 0, t) \qquad \text{as} \qquad e_\gamma \to 1 \tag{6.42}$$

at each point (x, y) of the intersection between the exact contact region $\mathscr{D}(t)$ and its approximation $\mathscr{D}_{(2)}(t)$ with the boundary (6.38). The hydrodynamic force on the entering body is given within strip theory by the formula

$$F_{(2)}(t) = \frac{\mathrm{d}}{\mathrm{d}t}\left(\frac{\pi}{2}\rho U_0 \int_{-b_{(2)}(t)}^{b_{(2)}(t)} \bar{a}^2(t, y)\mathrm{d}y\right) \tag{6.43}$$

which yields after calculations

$$F_{(2)}(t) = 2\pi\rho A^2 B U_0^2\sqrt{U_0t}. \tag{6.44}$$

The exact formula for the hydrodynamic force on the entering elliptic paraboloid follows from equations (4.12), (4.13), (6.13) and (6.14):

$$F(t) = \pi\rho B^3 U_0^2\sqrt{U_0t}\,\frac{1 - e^2}{E(e)}\left[1 + k^2\frac{D(e)}{E(e)}\right]^{3/2}. \tag{6.45}$$

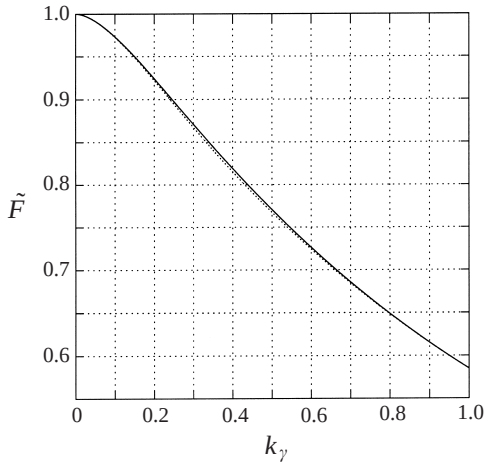

FIGURE 17. The ratio $\tilde{F}(k_\gamma)$ between the hydrodynamic force, $F(t)$, given by the Wagner theory and that, $F_{(2)}(t)$, by the strip theory, as function of the aspect-ratio factor k_γ of the entering elliptic paraboloid. Solid line corresponds to the exact formula (6.47) and the dotted line to the approximate formula (6.48).

With the help of equation (6.15), we obtain

$$F(t) = F_{(2)}(t)\tilde{F}(A/B), \tag{6.46}$$

$$\tilde{F}(k_\gamma) = \frac{3\sqrt{3}}{2E(e)} \frac{k^2/k_\gamma^2}{[k^2/k_\gamma^2 + 1]^{3/2}}, \quad k_\gamma = \frac{A}{B}. \tag{6.47}$$

The function $\tilde{F}(A/B)$ is depicted in figure 17. It is seen that $\tilde{F}(A/B) \to 1$ as $A/B \to 0$. More details can be obtained using the approximate formula (6.16), which gives

$$\tilde{F}(k_\gamma) \approx \frac{(2 + k_\gamma^2)\sqrt{1 + 2k_\gamma^2}}{2E(e)(1 + k_\gamma^2)^{3/2}}, \quad e = \sqrt{\frac{1 - k_\gamma^4}{1 + 2k_\gamma^2}}. \tag{6.48}$$

We conclude that $\tilde{F}(k_\gamma) = 1 + O(k_\gamma^2)$ for elongated bodies, $k_\gamma^2 \to 0$ and $\tilde{F}(1) = 1/\pi(3/2)^{3/2} \approx 0.585$ in the axisymmetric case. Figure 17 shows a very small discrepancy between the exact (6.47) and approximate (6.48) expressions for $\tilde{F}$. We conclude that in the case of an elliptic paraboloid, strip theory can be safely used to evaluate the hydrodynamic force on the entering body (10% discrepancy) when $A < B/4$.

7. Conclusion

The inverse method has been used to construct solutions of the impact problem using the Wagner approach. Within the framework of the inverse Wagner problem the body velocity and the contact line between the liquid free surface and the surface of the entering body are given, and we can determine the body shape and the liquid flow. The method provides a wide range of exact analytical solutions in the case of an elliptic contact region. It is proved that an elliptic paraboloid entering the liquid either with a constant velocity or with a constant acceleration has an elliptic contact region. It is shown how the inverse method can be used at the design stage. Experiments with body shapes analysed in this paper, are planned. The analytical solutions obtained are used to analyse the approach to the impact problem based on strip theory.

The results of this paper are helpful both for the comparison and validation of other approaches and for direct industrial application. They can be used to estimate the slamming loads on structures with compound curvature for design purpose, for example on the bow flare of FPSO and the stern part of a cruiser. The inverse method can be used to solve the direct problem of impact only for simple shapes. In general case other methods have to be employed.

The main obstacle to solving accurately the direct Wagner problem is closely connected to the fact that this problem is nonlinear, despite the linearization of both the equations of motion and the boundary conditions. The nonlinearity comes from the Wagner condition which is the main feature of this approach. In order to develop a general method to solve accurately the direct Wagner problem, we suggest linearizing this problem on the basis of a known analytical solution and studying the linearized problem first. The linearization can be carried out with the help of the displacement potential instead of the velocity potential utilized in the present paper. The linearized Wagner problem will be used to study the water entry problem for almost axisymmetric bodies in Part 2 of our work, currently in preparation. Another possibility is to linearize the original Wagner problem on the basis of the exact analytical solutions obtained in the present paper.

The next step is to consider the linearization of the Wagner problem on the basis of a solution obtained numerically (for example, on the basis of the solution described in § 5.1). This part of our work, Part 3 (also in preparation), is aimed at studying the stability of particular solutions and optimizing the shape of a body subject to water impact. The results of this research lead to a time-marching procedure, which will enable the impact problem to be solved for smooth bodies of an arbitrary shape. It is important to note that the procedure does not require iterations of the contact lines.

The problem of impact of non-smooth bodies, for example, pyramid- or star-shaped ones, which are of practical interest, requires special attention. We intend to develop further the inverse method with the help of functional transforms of harmonic functions and to derive exact solutions of the Wagner problem for contact regions with corner points. With these exact solutions to hand, it will be possible to study the linearized Wagner problem for non-smooth bodies and to develop suitable numerical algorithms to solve the original Wagner problem.

Mathematical analysis of regularity properties of the solutions of the Wagner problem would be highly desirable. These properties have to be taken into account for developing accurate and economical numerical algorithms.

The main part of this work was carried out at the Lavrentyev Institute of Hydrodynamics, Novosibirsk, during a sabbathical leave of Y.-M. S. from April to June 1999. This visit was supported by the Conseil Général des Bouches du Rhône (France) and by an industrial CEPM contract with partners Bureau Veritas, Institut Français du Pétrole and Principia RD. Results of § 5.3 were presented at the 15th International Workshop on Water Waves and Floating Bodies, Dan Caesarea, Israel, 2000. A. A. K. acknowledges the support from RFBR (projects No. 00-01-00839 and No. 00-15-96162) and SB RAS (integrated grant No. 1).

Appendix. Limit analysis for the velocity potential on an elliptic disk

In this Appendix the limit of the coefficient C in equation (4.5) is determined from the boundary condition (4.7) as $c \to 0$. The boundary condition on the body is first

transformed in terms of the ellipsoidal coordinates

$$\varphi_{,\lambda} = -Uz_{,\lambda} \quad \text{at} \quad \lambda = 0, \tag{A 1}$$

where

$$\varphi_{,\lambda} = Cz_{,\lambda} \int_{\lambda}^{\infty} \frac{\mathrm{d}\xi}{(c^2+\xi)^{3/2} g(\xi)} - \frac{Cz}{(c^2+\lambda)^{3/2} g(\lambda)} \tag{A 2}$$

for $\lambda > 0$ as follows from equation (4.5). Using the equality (see § 4)

$$z_{,\lambda} = \frac{z}{2(c^2+\lambda)} \tag{A 3}$$

and equation (A 2), we present the boundary condition (A 1) in the form

$$\lim_{\lambda \to +0} z_{,\lambda} \left[C \int_{\lambda}^{\infty} \frac{\mathrm{d}\xi}{(c^2+\xi)^{3/2} g(\xi)} - \frac{2C}{(c^2+\lambda)^{1/2} g(\lambda)} + U \right] = 0. \tag{A 4}$$

Taking into account that

$$\lim_{\lambda \to +0} z_{,\lambda} \neq 0 \tag{A 5}$$

in (A 4), the following equation is obtained:

$$C \lim_{\lambda \to +0} \left[\int_{\lambda}^{\infty} \frac{\mathrm{d}\xi}{(c^2+\xi)^{3/2} g(\xi)} - \frac{2}{(c^2+\lambda)^{1/2} g(\lambda)} \right] = -U \tag{A 6}$$

for the coefficient C. It is seen that difficulties may occur when both c and λ vanish. In order to avoid these, we integrate in (A 6) by parts and arrive at the following equation, where the singularity of the integrand has been removed:

$$U = 2C \lim_{\lambda \to +0} \int_{\lambda}^{\infty} \frac{g'(\xi)\mathrm{d}\xi}{(c^2+\xi)^{1/2} g^2(\xi)}. \tag{A 7}$$

We can now take the limit in (A 7) when $\lambda \to 0$ and $c \to 0$ and decompose the resulting integral into two standard ones:

$$I_1 = \int_0^{\infty} \frac{\mathrm{d}\xi}{\sqrt{\xi(\xi+a^2)^3(\xi+b^2)^3}} \tag{A 8}$$

and

$$I_2 = \int_0^{\infty} \frac{\sqrt{\xi}\mathrm{d}\xi}{\sqrt{(\xi+a^2)^3(\xi+b^2)^3}}. \tag{A 9}$$

The first one, I_1, is given as (see Gradshteyn & Ryzhik 1994, 3.135.4)

$$I_1 = \frac{2}{e^4 a^2 b^5} \left[(a^2+b^2)E(e) - 2a^2 K(e) \right], \tag{A 10}$$

where the elliptic functions $E(e)$ and $K(e)$ are defined in §§ 4 and 6, respectively. The second integral is first transformed into

$$I_2 = \int_0^{\infty} \frac{\mathrm{d}\xi}{\sqrt{\xi(\xi+a^2)(\xi+b^2)^3}} - a^2 I_1 = I_3 - a^2 I_1, \tag{A 11}$$

where the integral I_3 is equal to

$$I_3 = \frac{2}{(b^2-a^2)b} \left(K(e) - E(e) \right). \tag{A 12}$$

Substituting I_1, I_2 and I_3 into (A 7) with correct coefficients, we obtain the final result as

$$C = \frac{Ua^2 b}{2E(e)}. \tag{A 13}$$

REFERENCES

Abramowitz, M. & Stegun, I. A. 1979 *Handbook of Mathematical Functions*. Dover.

Appell, P. 1932 *Traité de Mécanique Rationnelle Tome Quatrième: Fascicule, Figures d'Équilibre d'une Masse Liquide Homogène en Rotation*. Gauthier-Villars.

Bisplinghoff, R. L., Ashley, H. & Halfman, R. L. 1996 *Aeroelasticity*. Dover.

Borodich, F. M. 1988 Similarity in the three-dimensional penetration problem of solid bodies into an ideal incompressible fluid. *Z. Prikl. Mekh. Tekh. Fiz.* **5**, 127–132 (English translation from the Russian).

Donguy, B., Peseux, B. & Fontaine, E. 2000 On the ship structural response due to slamming loads. *European Congress on Computational Methods in Applied Sciences and Engineering, ECCOMAS 2000, Barcelona, 11-14 September 2000*. CIMNE Barcelona Publication.

Glauert, H. 1983 *The Elements of Aerofoil and Airscrew Theory*. Cambridge University Press.

Gradshteyn, I. S. & Ryzhik, I. M. 1994 *Tables of Integrals*, 5th Edn. Academic.

Hauptmann, A. & Miloh, T. 1986 On the exact solution of the linearized lifting-surface problem of an elliptic wing. *Q. J. Mech. Appl. Maths* **39**, 41–66.

Howison, S. D., Ockendon, J. R. & Wilson, S. K. 1991 Incompressible water-entry problems at small deadrise angles. *J. Fluid Mech.* **222**, 215–230.

Korobkin, A. A. 1982 Formulation of penetration problem as a variational inequality. *Din. Sploshnoi Sredy* **58**, 73–79.

Korobkin, A. A. 1985 Initial asymptotics of solution of three-dimensional problem on a blunt body penetration into ideal liquid *Dokl. Akad. Nauk SSSR* **283**, 838–842.

Korobkin, A. A. 1994 Blunt-body penetration into a slightly compressible liquid. In *Proc. 20th Symp. on Naval Hydrodynamics, Santa Barbara*, vol. 3, pp. 179–186. Office of Naval Research.

Korobkin, A. A. 1996 Elastic effects on slamming. *Rep.* NAOE-96-39. University of Glasgow.

Korobkin, A. A. 1997 *Liquid-Solid Impact*. Novosibirsk, Siberian Branch of the Russian Academy.

Korobkin, A. A. & Pukhnachov, V. V. 1988 Initial stage of water impact. *Ann. Rev. Fluid Mech.* **20**, 159–185.

Lamb, H. 1932 *Hydrodynamics*. Cambridge University Press.

Leonov, M. Ya. 1940 Problems and applications of the theory of potential. *J. Appl. Maths Mech., USSR Acad. Sci.* **IV**(5–6), 73–86.

Meyerhoff, W. K. 1970 Added masses of thin rectangular plates calculated from potential theory. *J. Ship Res.* (June), 100–111.

Milne-Thomson, L. M. 1960 *Theoretical Hydrodynamics*, 4th Edn. McMillan & Co. Ltd.

Molin, B., Cointe, R. & Fontaine, E. 1996 On energy arguments applied to the slamming force. In *Proc. 11th Workshop on Water Waves and Floating Bodies, Hamburg, 17–20 March 1996* (ed. V. Bertram).

Pabst, W. 1930 Theorie des Landestosses von Seeflugzeugen. *Z. Flugtech. Motorluftschiff.* **21**, 217–226.

Schmieden, C. 1953 Der Aufschlag von Rotationskörpern auf eine Wasseroberfläche. *Z. Angew. Math. Mech.* **33**(4), 147–151.

Scolan, Y.-M. 1999 Slamming on an elliptic paraboloid. Self-similar solution and inverse problem. *Internal Rep. Lavrentyev Institute of Hydrodynamics*.

Scolan, Y.-M. & Korobkin, A. A. 2000 Design of three-dimensional bodies subject to water impact. In *Proc. 15th Workshop on Water Waves and Floating Bodies, Dan Caesarea, Israel* (ed. T. Miloh & G. Zilman), pp. 162–165.

Shiffman, M. & Spenser, D. C. 1951 The force of impact on a cone striking a water surface (vertical entry). *Commun. Pure Appl. Maths* **4**(4), 379–417.

Takagi, K. 1997 Three-dimensional slamming of a distorted plate. *Proc. ISOPE Symp. Hawaii*, vol. 1, pp. 237–244.

Toyama, Y. 1996 Flat plate approximation in the three-dimensional slamming. *J. Soc. Naval Arch. Japan* **179**, 271–279.

Tuck, E. O. 1993 Some accurate solutions of the lifting surface integral equation. *J. Austral. Math. Soc.* B **35**, 127–144.

Wagner, H. 1932 Über Stoss- und Gleitvorgänge an der Oberfläche von Flüssigkeiten. *Z. Angew. Math. Mech.* **12**, 193–215.

Watanabe, I. 1986*a* On hydrodynamic impact pressure acting upon flat bottomed ships. *J. Soc. Naval Arch. Japan* **159**, 201–210.

Watanabe, I. 1986*b* Theoretical investigation on the wave impact loads on ships. In *Proc. 16th Symp. on Naval Hydrodynamics, Berkeley*. Office of Naval Research.

Watanabe, I. 1987 Effects of the three-dimensionality of ship hull on the wave impact pressure. *J. Soc. Naval Arch. Japan* **162**, 163–174.

Wood, D. J. 1997 Pressure-impulse impact problems and plunging wave jet impact. PhD dissertation, University of Bristol.

Zaremba, S. 1910 Sur un problème mixte relatif à l'équation de Laplace. *Bull. Acad. Sci. Cracovie: Sci. Maths Naturelles* A, 313–344.